A Measure Theoretic Approach to Image Segmentation Framed in Terms of Intensities

Bachelor's Thesis

based on the course *Numerische Mathematik I*

Institut für Mathematik und wissenschaftliches Rechnen
Universität Graz

Daniel Kraft

Supervisor: a.o. Univ.-Prof. Mag. Dr. Stephen Keeling

Abstract

For the case of gray-scale images, we will formulate the problem of image segmentation based on the distribution of intensities in the image interpreted in a probabilistic sense. This leads to a finite-dimensional optimization problem, for which the optimality system will be derived and discussed. Application of a fixed-point iteration to this system leads to the well-known k-means clustering algorithm, for which this therefore is a measure theoretic justification and derivation. The reformulation also enables very efficient computation for common image representations, where the time-complexity does not depend on the image's size. Finally, the effect of random noise added to the original image will be discussed; this fits in naturally with the probabilistic framework and it will be shown that a noisy image satisfies nice smoothness conditions.

September 1st, 2010

Contents

1 Introduction

In mathematical image processing, an image can be modeled as a function that maps some domain Ω, that is a subset of the plane $\mathbb{R}^2$ for an "image" in the classical sense, to "colours" or intensities. In my thesis, I will only consider the case of *gray-scale* images, i.e., some interval $I \subset \mathbb{R}$ as range. The elements of I are the possible *intensities* for points of the image; usually they are represented in the applications either as floating-point numbers in the range $[0, 1]$ or integer numbers in some range $[0, 2^n - 1]$. So I will further require that I is bounded and can thus be represented as compact interval of real numbers. In addition, I need some technical requirements with regards to measurability.

Definition 1. Let $(X, \mathcal{F}, \mu)$ be a measurable space (typically, $(\mathbb{R}^2, \mathcal{L}, \lambda)$ with λ being the two-dimensional Lebesgue measure), $\Omega \in \mathcal{F}$ with $|\Omega| < \infty$ (finite measure) and $u : \Omega \to \mathbb{R}$ a bounded mapping. Note that for brevity, $|A|$ will denote $\mu(A)$ for $A \in \mathcal{F}$. For a subset $\omega \subset \Omega$, we say that its *image* under u is $u(\omega) = \{u(x) \mid x \in \omega\}$; similarly, for $J \subset I$, its *preimage* is $u^{-1}(J) = \{x \in \Omega \mid u(x) \in J\}$.

Let u be measurable (i.e., for all Borel-sets $B \in \mathcal{B}$ with $B \subset I$ we have $u^{-1}(B) \in \mathcal{F}$) and define $I^- = \inf u(\Omega)$ and $I^+ = \sup u(\Omega)$. As u is bounded, clearly $-\infty < I^- \leq I^+ < \infty$. u is said to be an *image* on Ω with intensities in $I = [I^-, I^+]$, if $I^- < I^+$ and for all $I^- < t < I^+$ we have

$$\left|u^{-1}\left([I^-, t]\right)\right| \neq 0 \neq \left|u^{-1}\left([t, I^+]\right)\right|. \tag{1}$$

If $u, u' : \Omega \to I$ are two images with $u = u'$ almost everywhere (i.e., $|\{x \in \Omega \mid u(x) \neq u'(x)\}| = 0$), I'll identify u and u', considering them to represent the same image. Thus strictly speaking, each *image* will mean the equivalence class of all functions identified with it. Note that by this identification, we can without loss of generality assume that for each bounded mapping u Equation 1 holds. The other condition imposed in Definition 1, namely $I^- < I^+$, just excludes the trivial case of a constant u which will not be considered in the following.

Now we can formulate and show the following easy technical result. For this, recall that $\mathrm{L}^2(\Omega, I)$ is the space of equivalence classes of Lebesgue square-integrable functions mapping $\Omega \to I$. This is a Banach-space with the norm

$$\|f\|_{\mathrm{L}^2} = \left(\int_\Omega |f|^2 \, d\mu\right)^{\frac{1}{2}}.$$

See [3, p. 80ff] for more details and [3, p. 85, 2.4.11] for a proof of completeness.

Lemma 1. *Let $u : \Omega \to I$ be an image. Then $u \in L^2(\Omega, I)$.*

Proof. Per definition, u is an equivalence class of Lebesgue measurable functions mapping $\Omega \to I$. Because $\int_\Omega |u|^2 \, d\mu \leq |\Omega| \max_{t \in I} |t|^2 < \infty$, the assertion follows. □

Given an image, the process of *segmentation* tries to divide its domain into a small number of *subdomains* in such a way that they correspond as well as possible to qualitatively distinct areas in the image. Those areas may be associated to separate objects depicted in the image, for instance, but are usually meant to be of a more or less uniform intensity. Thus more strictly, segmentation can be understood as looking for an approximation to the image u by a step-function s. My goal in this work is to derive a way to find a good such approximation s for a given image u.

Definition 2. Let $u : \Omega \to I$ be an image and $M \in \mathbb{N}^+$. Then a M segment *segmentation* of u is a step-function $s : \Omega \to I$ of the form

$$s = \sum_{i=1}^{M} c_i \chi_{\Omega_i},$$

where $c_i \in I$ are the *segment intensities*, $\Omega_1, \ldots, \Omega_M$ is a partition of Ω (i.e., Ω is the disjoint union of all Ω_i and all Ω_i are non-empty) and χ_{Ω_i} denotes the characteristic function of Ω_i, where

$$\chi_A(x) = \begin{cases} 1 & x \in A \\ 0 & x \notin A \end{cases}$$

for some set $A \subset \Omega$. The sets Ω_i will be called the *segments* of u in this segmentation. This segmentation s can also be specified as the set $\{(\Omega_1, c_1), \ldots, (\Omega_n, c_M)\}$, which means the same thing. In addition to requiring $\Omega_i \neq \emptyset$, we will further require that $|\Omega_i| > 0$ for all i, as changes on a set of measure zero are not interesting.

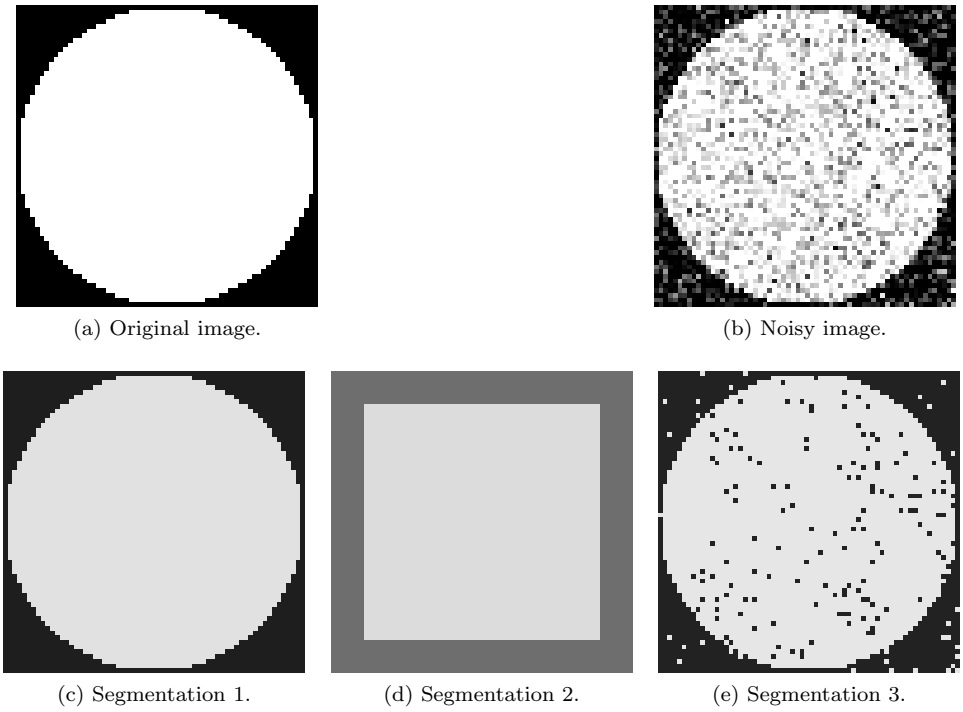

(a) Original image. (b) Noisy image.

(c) Segmentation 1. (d) Segmentation 2. (e) Segmentation 3.

Figure 1: Basic example of image segmentations.

For two segmentations s, s' of the image u, we say that s is *better* than s' iff $\|s-u\|_{\mathrm{L}^2} < \|s'-u\|_{\mathrm{L}^2}$. In this way, we can clearly define a total ordering on the family of all segmentations of u. I'll refer to the dimension-less constant

$$\epsilon = \frac{\|s-u\|_{\mathrm{L}^2}}{\|u\|_{\mathrm{L}^2}}$$

as the *quality* or *relative error* of the segmentation s of an image u later on.

Image segmentation has a wide variety of applications in image processing, both as a step that is useful on its own, but also as regularization inside some larger processing-algorithm, as in [8]. See also [4, ch. 4].

Given just a partition of Ω as $\Omega_1, \ldots, \Omega_M$, it seems intuitive to define c_i as some "mean value" of u over the set Ω_i for $i = 1, \ldots, M$ to get a full segmentation. This will be discussed later in more detail (see *Theorem* 2), but let it suffice for now to state this informally.

Finally, in Figure 1 I've assembled some examples about image segmentation. Figure 1a is an original black-and-white image, which got corrupted by noise in Figure 1b. In the bottom row, I've shown three different segmentations of Figure 1b with two segments each, where the segment intensities are always the mean values over the two sub-domains, but the choice of sub-domains is different.

For Figure 1c, the two sub-domains are the ones in the original image; naturally, this segmentation looks quite similar to the original. The relative error is 0.22. In Figure 1d, the sub-domains are obviously poorly chosen, but this is still a possible segmentation (although not a very good one, the relative error is 0.39). The sub-domains in Figure 1e are chosen such that pixels with intensity in $[0, \frac{1}{2}]$ are in one and those with intensity in $(\frac{1}{2}, 1]$ in the other. This is also a reasonable choice, and its relative error is only 0.18, so by this criterion the best segmentation.

Most will probably agree that the "natural" segmentation is nevertheless Figure 1c because the noisy image still clearly consists of a circle on a background, and thus the artefact pixels in Figure 1e seem unnatural. But to notice this, one has to consider the image as a whole and take geometric properties of the segments into consideration (like trying to regularize their boundaries). My definition of segment quality and also the considerations in the following are by contrast purely based on the intensities of the individual pixels, no matter how those pixels are situated relative to each other. This is motivated by the concept of topological derivatives which will be described in Section 2 below, but there are also segmentation strategies that, e.g., penalize irregular segment boundaries to avoid effects like this; see for instance [7, p. 18ff].

2 Topological Derivatives, "Best" Segmentations

As a next step, I will try to characterize "best" segmentations (in the sense of the ordering in Definition 2). First, let's consider a given partition of the image domain $\Omega_1, \ldots, \Omega_M$; then we can find an easy (and intuitive) result about the optimal intensities c_i in this case (see also [7, p. 4]):

Theorem 2. *Let $u : \Omega \to I$ be an image and $\Omega_1, \ldots, \Omega_M$ a partition of Ω with $|\Omega_i| > 0$ for $i = 1, \ldots, M$. Then $\{(\Omega_i, c_i) \mid i = 1, \ldots, M\}$ with*

$$c_i = \frac{1}{|\Omega_i|} \int_{\Omega_i} u \, d\mu \tag{2}$$

has the best quality among all segmentations $\{(\Omega_i, d_i) \mid i = 1, \ldots, M\}$ for $d_1, \ldots, d_M \in I$. The optimal intensities c_i are the unique minimizer.

Proof. Let $F : \mathbb{R}^M \to \mathbb{R}$ be the function mapping a set of intensities $(c_1, \ldots, c_M)$ to the square of the corresponding segmentation error, i.e.,

$$F(c_1, \ldots, c_n) = \sum_{i=1}^{M} \int_{\Omega_i} (u - c_i)^2 \, d\mu.$$

Note that the c_i need not be in I for the definition of F, thus F can be defined on the whole of $\mathbb{R}^M$. Then clearly the segmentation with intensities $(c_1, \ldots, c_M)$ is better than that with intensities $(d_1, \ldots, d_M)$, iff $F(c_1, \ldots, c_M) < F(d_1, \ldots, d_M)$. Thus we have to prove that the choice of c_i according to Equation 2 minimizes F. F is obviously a twice continuously differentiable function, and we get

$$\frac{\partial F}{\partial c_i} = -2 \left(\int_{\Omega_i} u \, d\mu - c_i \, |\Omega_i| \right).$$

Thus $\nabla F = 0$ if and only if c_i satisfies Equation 2 for all i, so this is the only critical point. To establish that it actually is a minimum, consider the Hessian of F. The second partial derivatives are

$$\frac{\partial^2 F}{\partial c_j \partial c_i} = 2 \, |\Omega_i| \, \delta_{ij},$$

thus the Hessian is diagonal and positive definite, since $|\Omega_i|$ is assumed to be positive for all $i = 1, \ldots, M$. □

It should be intuitively clear that splitting a segment will result in a new segmentation with quality at least as good, which is formalized as follows:

Lemma 3. *Let $\{(\Omega_i, c_i) \mid i = 1, \ldots, M\}$ be a segmentation and let $\Omega_j = A \dot\cup B$ be the disjoint union of two non-empty sets A and B with $|A| \neq 0 \neq |B|$. Then there exists a segmentation with the sub-domains $\Omega_1, \ldots, \Omega_{j-1}, A, B, \Omega_{j+1}, \ldots, \Omega_M$ that has quality at least as good.*

Proof. If we define the new segmentation as $\{(\Omega_i, c_i) \mid i \neq j\} \cup (A, c_j) \cup (B, c_j)$, this is clearly equivalent to the original segmentation in terms of quality. Note however, that in general this segmentation has not optimal intensities for its sub-domains (as by Theorem 2) and thus we can usually adapt the intensities and get a segmentation with even higher quality than the original one. □

For analysis of optimal sub-domains, the concept of *topological derivatives* is useful. Basically, given a segmentation s represented by $\{(\Omega_i, c_i) \mid i = 1, \ldots, M\}$, two indices $i, j = 1, \ldots, M$ and $x \in \Omega_i$, the topological derivative $\mathcal{T}_{ij}(x)$ of the segmentation is defined according to

$$\mathcal{T}_{ij}(x) = \lim_{\rho \to 0} \frac{1}{|\mathcal{B}_\rho(x)|} \left(\|u - s_\rho\|_{\mathrm{L}^2}^2 - \|u - s\|_{\mathrm{L}^2}^2 \right)$$

with s_ρ being the segmentation represented by the changed segments

$$\{(\Omega_1, c_1), \ldots, (\Omega_i \setminus \mathcal{B}_\rho(x), c_i), \ldots, (\Omega_j \cup \mathcal{B}_\rho(x), c_j), \ldots, (\Omega_M, c_M)\}.$$

$\mathcal{B}_\rho(x)$ stands for the ball around x with radius ρ. Thus, $\mathcal{T}_{ij}(x)$ describes how the segmentation error changes when transferring "the point x" from segment i to segment j. This is described in more detail in [7, p. 6f]; there is also shown that

$$\mathcal{T}_{ij}(x) = \begin{cases} (u(x) - c_j)^2 - (u(x) - c_i)^2 & |\Omega_j| > 0 \\ -(u(x) - c_i)^2 & |\Omega_j| = 0 \end{cases}, \tag{3}$$

if the intensities of the segmentation satisfy Equation 2. So if for some i, j and $\omega \in \Omega_i$ we have $\mathcal{T}_{ij}(x) < 0$, the choice of sub-domains Ω_i and Ω_j is sub-optimal. (Or put another way, for an optimal segmentation, we can expect that $\mathcal{T}_{ij}(x) \geq 0$ for all i, j and $x \in \Omega_i$.)

From a practical point of view, it makes sense that all segments in a segmentation have different intensities. Otherwise, segments with the same intensity can be joined. Also — at least when only considering the individual pixels and not their neighbourhoods, as I do — no two sub-domains should contain pixels in which the original image assumes the same intensity. Otherwise, we can just put all of them into one of those segments. Thus, the we want the following conditions to hold true:

$$\forall i \neq j \quad : \quad c_i \neq c_j, \tag{4}$$

$$u(\Omega_i) \cap u(\Omega_j) = \emptyset \tag{5}$$

Lemma 4. *If s represented by $\{(\Omega_i, c_i) \mid i = 1, \ldots, M\}$ is a segmentation of the image u, there exists a segmentation s' satisfying Equation 4 and Equation 5 while not having more segments and not less quality than s.*

Proof. Assume that Equation 4 is violated and let $i, j = 1, \ldots, M$ be with $c_i = c_j$. Then clearly

$$\int_{\Omega_i} (u - c_i)^2 \, d\mu + \int_{\Omega_j} (u - c_j)^2 \, d\mu = \int_{\Omega_i \cup \Omega_j} (u - c_i)^2 \, d\mu$$

and thus $\|u - s\|_{\mathrm{L}^2} = \|u - s'\|_{\mathrm{L}^2}$ with s' represented by $\{(\Omega_k, c_k) \mid k \notin \{i, j\}\} \cup \{(\Omega_i \cup \Omega_j, c_i)\}$. So we can ensure Equation 4, whether Equation 5 holds or not. Assume from now on that Equation 4 holds, i.e., that $c_i \neq c_j$ for all i, j.

If Equation 5 is violated, define for $i = 1, \ldots, M$ the sets

$$B_i = \{x \in \Omega \mid \forall j < i : \ |u(x) - c_i| < |u(x) - c_j| \ \text{ and } \forall j > i : \ |u(x) - c_i| \leq |u(x) - c_j|\}. \tag{6}$$

It is clear that $|u(x) - c_i| \leq |u(x) - c_j|$ for all $x \in B_i$ and $i, j = 1, \ldots, M$. Suppose that $x \in B_i \cap B_j$ with $i < j$. Then $|u(x) - c_i| = |u(x) - c_j|$ but this is a contradiction to $x \in B_j$. Thus all B_i, $i = 1, \ldots, M$, are disjoint. For $x \in \Omega$ arbitrary, the finite set $\{|u(x) - c_i| \mid i = 1, \ldots, M\}$ has a minimum; if we choose $k \in \{1, \ldots, M\}$ minimal such that $|u(x) - c_i| = |u(x) - c_k|$, then $x \in B_k$. Thus we get

$$\Omega = B_1 \dot{\cup} \ldots \dot{\cup} B_M.$$

Because the condition on x in Equation 6 does only depend on $u(x)$, it can be shown similarly to the argument above that Equation 5 holds for the sets $B_1, \ldots, B_M$. We can now define a new segmentation $s' = \{(B_i, c_i) \mid i = 1, \ldots, M\}$. This satisfies Equation 5 and has as many segments as s. It is also not worse because of:

$$\|u - s\|_{\mathrm{L}^2}^2 = \sum_{i,j=1}^{M} \int_{\Omega_i \cap B_j} (u - c_i)^2 \, d\mu \geq \sum_{i,j=1}^{M} \int_{\Omega_i \cap B_j} (u - c_j)^2 \, d\mu = \|u - s'\|_{\mathrm{L}^2}^2$$

□

Note that the intensities c_i' of the new segmentation s' from Lemma 4 need not necessarily satisfy Equation 2. However, once a segmentation s' is obtained satisfying Equation 4 and Equation 5, then according to Theorem 2 the intensities of s' can be adjusted by Equation 2 to obtain the best quality. So from now on, when looking for a good segmentation with few different intensities, we can concentrate only on segmentations s' that satisfy those conditions.

Theorem 5. *Let $s = \{(\Omega_i, c_i) \mid i = 1, \ldots, M\}$ be a segmentation of the image u satisfying Equation 4 and Equation 5 such that c_i satisfies Equation 2 for $i = 1, \ldots, M$. Also assume that s is not perfect, i.e., $s \neq u$. If all topological derivatives are non-negative, then there exists a partition of I into non-empty disjoint intervals $I_1, \ldots, I_M$ such that $\Omega_i = u^{-1}(I_i)$ for all $i = 1, \ldots, M$.*

Proof. It will first be shown that $\Omega_i \neq \emptyset$ for all $i = 1, \ldots, M$: Assume that $\Omega_i = \emptyset$. Because $s \neq u$, there exists j and $x \in \Omega_j$ such that $u(x) \neq c_j$. But then according to Equation 3, $\mathcal{T}_{ji}(x) < 0$ which contradicts the assumption on the topological derivatives. For all $k = 1, \ldots, M$, $\Omega_k \neq \emptyset$ also means that $u(\Omega_k) = I_k \neq \emptyset$.

Next, define $J_k = u(\Omega_k)$ for $k = 1, \ldots, M$. Then according to Equation 5 all J_k are disjoint and obviously $J_k \subset I$. I'll show that for all $i, j = 1, \ldots, M$, either $\sup J_i \leq \inf J_j$ or the other way round

(i.e., these sets are not interlaced). Assume this claim holds. Define $a_0 = \inf J_1$ and $a_i = \sup J_i$ for $i = 1, \ldots, M$, so that $a_0 \leq \ldots \leq a_M$. Then define

$$I_i = \begin{cases} (a_{i-1}, a_i) & a_{i-1} \in J_{i-1},\ a_i \notin J_i \\ [a_{i-1}, a_i) & a_{i-1} \notin J_{i-1},\ a_i \notin J_i \\ (a_{i-1}, a_i] & a_{i-1} \in J_{i-1},\ a_i \in J_i \\ [a_{i-1}, a_i] & a_{i-1} \notin J_{i-1},\ a_i \in J_i \end{cases} .$$

Then $J_i \subset I_i$ for $i = 1, \ldots, M$ and for all i, j, the intervals I_i and I_j are disjoint. Because $\cup_{i=1}^{M} I_i = [a_0, a_M]$ and since $I^- = \inf u(\Omega) = \min_k \inf J_k = a_0$ and $I^+ = a_M$, it follows that $\cup_{i=1}^{M} I_i = I$. Since $J_k \subset I_k$, it follows that $\Omega_k = u^{-1}(J_k) \subset u^{-1}(I_k)$ for $k = 1, \ldots, M$. Suppose there is an $x \in \Omega \setminus \Omega_k$ where $x \in u^{-1}(I_k)$. Then $x \in \Omega_l$ for some $l \neq k$ and $\Omega_l \cap u^{-1}(I_k) \neq \emptyset$. This means that $I_l \cap I_k = u(\Omega_l) \cap I_k \neq \emptyset$ which is a contradiction. Thus $\Omega_k = u^{-1}(I_k)$ for $k = 1, \ldots, M$ and the assertion is shown.

Assuming that the assertion about the sets J_i does not hold, there exist $i, j \in \{1, \ldots, M\}$, $a, c \in J_i$, $b \in J_j$ and $x, z \in \Omega_i$, $y \in \Omega_j$ such that $a = u(x), b = u(y), c = u(z)$ with $a < b < c$. Note that according to Equation 2, without loss of generality we can assume that $a \leq c_i \leq c$ because a and c can be chosen arbitrarily close to $\inf J_i$ and $\sup J_i$ and clearly $\inf J_i \leq c_i \leq \sup J_i$ holds; even strict inequalities if the infimum or supremum are not actually taken on.

There are two possible cases, firstly $a < b \leq c_i$ and secondly $c_i \leq b < c$. I'll only consider the first one, the second is similar. Because of the assumption on the topological derivatives, we know that $\mathcal{T}_{ji}(y) \geq 0$, which by Equation 3 and for non-empty Ω_i means that $(b - c_i)^2 \geq (b - c_j)^2$ or equivalently $|b - c_i| = c_i - b \geq |b - c_j|$.

If $c_j \leq b$, then $c_j \leq b \leq c_i$. If $b < c_j$, then $c_i - b \geq c_j - b$ again implies $c_j \leq c_i$. Because $c_i \neq c_j$, we get even $c_j < c_i$. Now if $a \leq c_j$, it follows that $|a - c_j| = c_j - a < c_i - a = |c_i - a|$ and thus also $\mathcal{T}_{ij}(x) < 0$ which is not possible. So let $c_j < a$. But then

$$|a - c_j| = a - c_j < b - c_j = |b - c_j| \leq |b - c_i| = c_i - b < c_i - a = |a - c_i| ,$$

which is a contradiction because it again means $\mathcal{T}_{ij}(x) < 0$. Thus, $a < b \leq c_i$ can not hold. □

Taking Theorem 2 and Theorem 5 together, we can represent "good" segmentations (in the sense of Equation 2, Equation 4 and Equation 5) by specifying only a partition of I into intervals I_k, $k = 1, \ldots, M$. Even more, we will see that under some additional assumptions on the image u (see Definition 4 and Equation 9 below) it does not matter for the segmentation's quality whether I_k contains its boundary points or not. Then, all information can be characterized by only giving the boundary points between those intervals. This amounts to a finite-dimensional vector (of $M - 1$ boundary points) and will lead to a finite-dimensional optimization problem, given in Equation 11 and analyzed in Section 4.

3 The Distribution and Cost Functions

3.1 Distribution

Definition 3. Let $u : \Omega \to I$ be an image and $(\Omega, \mathcal{F}, \mu)$ the underlying measurable space. Then define for $A \in \mathcal{F}$

$$\pi(A) = \frac{\mu(A)}{|\Omega|}.$$

This clearly makes $(\Omega, \mathcal{F}, \pi)$ a probability space, because π is a measure and additionally $\pi(\Omega) = 1$. On this probability space, u is also measurable and thus is a random variable. Let $p : \mathbb{R} \to \mathbb{R}$ be its cumulative distribution function.

By this definition, we get

$$p(t) = \pi(u^{-1}((-\infty, t])) = \frac{\left|u^{-1}((-\infty, t])\right|}{|\Omega|}.$$

Informally, the "random variable" in Definition 3 means "intensity of a randomly picked point in the image". Thus p represents a cumulative histogram of the image's intensities.

Lemma 6. *$p(\mathbb{R}) \subset [0, 1]$. p is monotonic increasing and continuous from the right. p is continuous from the left (thus continuous) in $t \in \mathbb{R}$ iff $\left|u^{-1}(\{t\})\right| = 0$.*

The function p has "compact support" in the sense that $p(t) = 0$ for all $t < I^-$ and $p(t) = 1$ for all $t \geq I^+$. On the other hand, $p(t) > 0$ for all $t > I^-$ and $p(t) < 1$ if $t < I^+$.

Proof. Most of this is well-known for distribution functions in general, see for instance [3, p. 209, 5.6.2].

Let $t < I^-$. Then $u^{-1}((-\infty, t]) = \emptyset$ and thus $p(t) = 0$. Similarly, for $t \geq I^+$, $u^{-1}((-\infty, t]) = \Omega$ and thus $p(t) = 1$. As a consequence of Definition 1 (in particular Equation 1), for every $t > I^-$ we have $\left|u^{-1}((-\infty, t])\right| > 0$ and thus $p(t) > 0$. For $t < I^+$, it follows similarly that $p(t) < 1$. □

Note that by Lemma 6, p is continuous if the image contains no positive measure regions of constant intensity; this means, it is more "photo-like" than "cartoon-like" and only has more or less steep gradients instead of constant intensity. On the other hand, p is constant in some interval $J \subset I$ if $\left|u^{-1}(J)\right| = 0$, since then for all $s, t \in J$ we have $p(t) - p(s) = \pi(u^{-1}((s, t]) = 0$.

Definition 4. p is said to be *natural*, if it is continuously differentiable and if $p'(t) > 0$ for all $t \in (I^-, I^+)$. Note that we actually need $p'(t) > 0$, requiring that p is strictly increasing is not enough.

In the following, I will often require that p is natural. This is certainly not true for all images, but we'll see in Section 5 that it is a reasonable assumption when the image u has some noise added to it (either directly because of its nature or even artificially to evade exactly this problem).

As per [3, p. 24, 1.4.4], p also gives rise to a Lebesgue-Stieltjes measure p on $\mathbb{R}$, with $p(A) = \pi(u^{-1}(A))$ for $A \in \mathcal{F}$. Integration over some interval with this measure can be interpreted as integration over its preimage under u in the original image domain:

Theorem 7. *Let $J \subset \mathbb{R}$ be an interval and $f : J \to \mathbb{R}$ be p-measurable. Then*

$$\int_J f \, dp = \frac{1}{|\Omega|} \int_{u^{-1}(J)} f \circ u \, d\mu. \tag{7}$$

Proof. Assume that $f(t) \geq 0$ for all $t \in J$. Otherwise this can be achieved by splitting f into positive and negative parts.

Now, per definition (see [3, p. 37]) of the Lebesgue-Stieltjes integral, we know that

$$\int_J f \, dp = \sup\left\{\int_J s \, dp \mid 0 \leq s \leq f, s \text{ simple}\right\}. \tag{8}$$

Let $s = \sum_{i=1}^n s_i \chi_{A_i}$ be a simple function satisfying $0 \leq s \leq f$ where A_i, $i = 1, \ldots, n$, is any partition of J. Then if we define $s' : u^{-1}(J) \to \mathbb{R}$ via $s'(x) = s(u(x))$, s' is also simple and $s' = \sum_{i=1}^n s_i \chi_{u^{-1}(A_i)}$. Clearly, for all $x \in u^{-1}(J)$ we have $s'(x) = s(u(x)) \leq f(u(x))$ and thus $0 \leq s' \leq f \circ u$. Then

$$\begin{aligned}\int_J s \, dp &= \sum_{i=1}^n s_i p(A_i) = \frac{1}{|\Omega|} \sum_{i=1}^n s_i \left|u^{-1}(A_i)\right| \\ &= \frac{1}{|\Omega|} \int_{u^{-1}(J)} s' \, d\mu \leq \frac{1}{|\Omega|} \int_{u^{-1}(J)} f \circ u \, d\mu.\end{aligned}$$

Because s was arbitrary, we get Equation 7 with "$\leq$". For the other way round, consider the analogue of Equation 8 for $f \circ u$ and let $s' = \sum_{i=1}^{n} s_i \chi_{B_i}$ be a simple function with $0 \leq s' \leq f \circ u$ for a partition B_i, $i = 1, \ldots, n$, of $u^{-1}(J)$. Define $s : J \to \mathbb{R}$ by $s(t) = \max_{x \in u^{-1}(\{t\})} s'(x)$. Then for all $t \in J$

$$s(t) = \max_{x \in u^{-1}(\{t\})} s'(x) \leq \sup_{x \in u^{-1}(\{t\})} f(u(x)) = f(t).$$

The sets $u(B_i)$ are a partition of J and for $t \in u(B_i)$, say $t = u(x)$ with $x \in B_i$, we have $s(t) \geq s'(x) = s_i$ because $x \in u^{-1}(\{t\})$. The general relation $u^{-1}(u(B_i)) \supset B_i$ implies that $p(u(B_i)) \geq \frac{|B_i|}{|\Omega|}$ and

$$\frac{1}{|\Omega|} \int_{u^{-1}(J)} s' \, d\mu = \sum_{i=1}^{n} s_i \frac{|B_i|}{|\Omega|} \leq \sum_{i=1}^{n} s_i p(u(B_i)) \leq \int_J s \, dp \leq \int_J f \, dp,$$

which gives Equation 7 with "$\geq$". □

Note that if u is sufficiently smooth, Theorem 7 can be understood in terms of the coarea formula [6, p. 118, Proposition 3]. Specifically, if $\mathcal{H}^1$ denotes the one-dimensional Hausdorff measure, then

$$\int_{-\infty}^{t} p'(s) \, ds = p(t) = \frac{1}{|\Omega|} \int_{u^{-1}((-\infty,t])} d\mu = \frac{1}{|\Omega|} \int_{-\infty}^{t} \left(\int_{u^{-1}(\{s\})} \frac{d\mathcal{H}^1}{|\nabla u|} \right) ds.$$

This implies that $p'(s) = \frac{1}{|\Omega|} \int_{u^{-1}(\{s\})} \frac{d\mathcal{H}^1}{|\nabla u|}$ and thus for $J = (\sigma, \tau]$ we get

$$\begin{aligned} \frac{1}{|\Omega|} \int_{u^{-1}(J)} f \circ u \, d\mu &= \frac{1}{|\Omega|} \int_{\sigma}^{\tau} \left(\int_{u^{-1}(\{s\})} \frac{f \circ u}{|\nabla u|} \, d\mathcal{H}^1 \right) ds \\ &= \int_{\sigma}^{\tau} f(s) \left(\frac{1}{|\Omega|} \int_{u^{-1}(\{s\})} \frac{d\mathcal{H}^1}{|\nabla u|} \right) ds = \int_J f \, dp. \end{aligned}$$

3.2 Cost Function

Definition 5. Let $J \subset \mathbb{R}$ be an interval with $p(J) > 0$. Then we define:

$$\begin{aligned} c_p(J) &= \frac{\int_J t \, dp(t)}{p(J)}, \\ F_p(J) &= \int_J (t - c_p(J))^2 \, dp(t). \end{aligned}$$

Note that both $c_p(J)$ and $F_p(J)$ are by now undefined if $p(J) = 0$! With Theorem 7, it is easy to see that

$$c_p(J) = \frac{\int_{u^{-1}(J)} u \, d\mu}{|u^{-1}(J)|}$$

if $\left|u^{-1}(J)\right| > 0$ and thus just corresponds to Equation 2 for the segment chosen as $u^{-1}(J)$. So if we define a segment as preimage of the interval J in intensity-space (as motivated in Section 2), its optimal intensity is given by $c_p(J)$. Similarly, rewritten as integration over the image domain we get

$$F_p(J) = \frac{1}{|\Omega|} \int_{u^{-1}(J)} (u - c_p(J))^2 \, d\mu.$$

This is just the segmentation error for that segment. Thus $F_p(J)$ (but summarized over all segments together of course, i.e., over J_i with $\cup_{i=1}^{n} J_i = I$) is to be minimized as our cost function later on; see Definition 6 below.

If p is natural, for any suitably measurable function f and interval $J \subset \mathbb{R}$ with boundary points $\sigma < \tau$ the relation

$$\int_J f \, dp = \int_{\sigma}^{\tau} f(t) p'(t) \, dt \tag{9}$$

holds. Especially, it does not matter whether the boundary points are part of the interval or not, because $\{\sigma, \tau\}$ has measure 0 with respect to the Lebesgue measure applied on the right-hand side in Equation 9. So in this case, we can without loss of generality assume that $J = (\sigma, \tau]$; this will be the standard form

for intervals defining segments via their preimages later on. Additionally, we can apply Equation 9 to reformulate Definition 5 based on p' and the ordinary Lebesgue measure. Because p is then also strictly increasing, all non-empty intervals have a positive p measure and the measure of an interval J as defined above is always $p(J) = p(\sigma) - p(\tau)$. We're finally able to define the set of possible segmentations that will be considered and then our cost function.

Definition 6. Let $u : I \to \mathbb{R}$ be an image and p the corresponding distribution function. Let p be natural. Then the simplex

$$B = \left\{ b \in \mathbb{R}^{M-1} \mid I^- = b_0 \leq b_1 \leq \cdots \leq b_{M-1} \leq b_M = I^+ \right\}$$

is the set of possible boundaries in intensity-space giving a segmentation of M segments by $\Omega_i = u^{-1}(J_i)$ with $J_i = (b_{i-1}, b_i]$.

Because p is increasing, $0 = p(J_i) = p(b_i) - p(b_{i-1})$ is equivalent to $b_i = b_{i-1}$. In this case, define now $c_p(J_i) = b_i$ and $F_p(J_i)$ in the usual way. For $b \in B$, our cost function is

$$K_p(b) = \sum_{i=1}^{M} F_p(J_i) = \sum_{i=1}^{M} \int_{b_{i-1}}^{b_i} (t - c_p(J_i))^2 p'(t)\, dt.$$

Lemma 8. *B is compact in $\mathbb{R}^{M-1}$ and the interior of B is the set*

$$B^\circ = \left\{ b \in \mathbb{R}^{M-1} \mid I^- = b_0 < b_1 < \ldots < b_M = I^+ \right\}. \tag{10}$$

Proof. B is clearly bounded. For compactness, I'll show that it is also closed. Let $\left(b^{(k)}\right) \subset B$ be a convergent sequence with limit $b \in \mathbb{R}^{M-1}$. Then for all $i = 1, \ldots, M-1$, $\lim_{k\to\infty} b_i^{(k)} = b_i$. Because for all $k \in \mathbb{N}$ per definition $b_{i-1}^{(k)} \leq b_i^{(k)}$ holds for $i = 1, \ldots, M$, this inequality is preserved by the limit and also $b_{i-1} \leq b_i$ holds, thus $b \in B$.

Now, define B' to be the set in Equation 10. Let $b \in B'$ be given and choose $0 < \epsilon < \frac{1}{2} \min_i (b_i - b_{i-1})$. Then it is easy to see that with respect to the $\|\cdot\|_\infty$ norm $\mathcal{B}_\epsilon(b) \subset B'$ holds, thus $B' \subset B^\circ$. On the other hand, assume $b \in B \setminus B'$. Then there exists i such that $b_i = b_{i+1}$; as a consequence, for any $\epsilon > 0$ the point $d = b + \epsilon e_i$ is in $\mathcal{B}_\epsilon(b)$ but $d \notin B$ as $d_i = b_i + \epsilon > b_{i+1} = d_{i+1}$. Thus, $b \notin B^\circ$ which finally implies $B' = B^\circ$. □

So in order to segment an image, we are solving the optimality problem:

$$K_p(b^*) = \min_{b \in B} K_p(b) \tag{11}$$

We'll see in Section 4 that K_p is continuous on B and continuously differentiable on its interior under the assumptions of Definition 6. Thus there is actually a solution to Equation 11. And because of the differentiability, we can look for that minimum based on the first order necessary optimality condition, which will result in Theorem 10.

3.3 Examples

In Figure 2 I've compiled three sample images together with their functions p and $K_p(b)$ for two and three intensities (which means that K_p is a function of one or two boundaries). It is clearly visible that for Figure 2b where the image itself is already piecewise constant, both p and K_p are discontinuous, while for the image Figure 2a and also the real image in Figure 2c the distribution and costs are smooth (except the discontinuity in Figure 2f at $t = 0$ because the image is placed on a black background).

The phantom image Figure 2b will be taken up again in Section 5 and Figure 4. There we will see that adding random noise to the image smoothes its corresponding functions, so that all theory done for continuously differentiable and strictly increasing p can be applied. But for now it suffices to notice that in the smooth case (and especially for real images like Figure 2c) the cost function is rather regular (although not necessarily convex as can be seen in Figure 2l) and thus easy to minimize — in the following (Section 4) I'll analyze this in theory and derive a suitable method for the optimization.

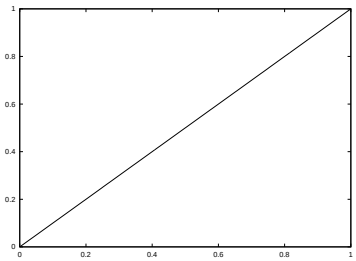

(a) 1D "image".

(b) Phantom image.

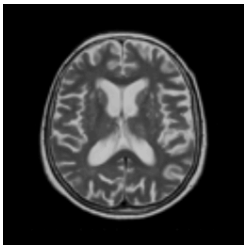

(c) Real image.

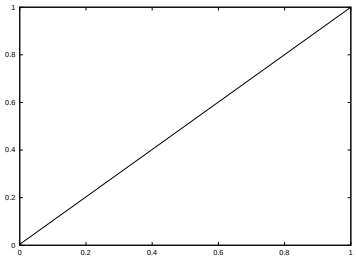

(d) Distribution p.

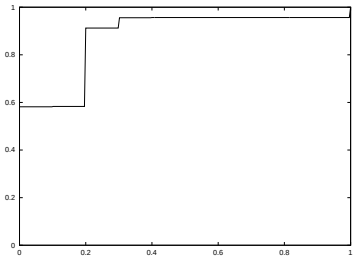

(e) Distribution p.

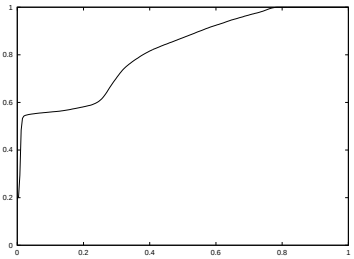

(f) Distribution p.

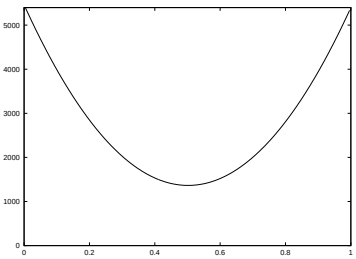

(g) Cost K_p for $M = 2$.

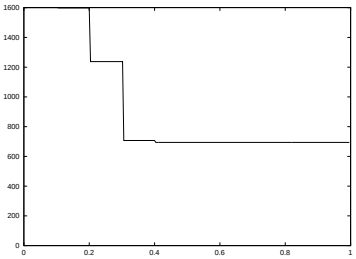

(h) Cost K_p for $M = 2$.

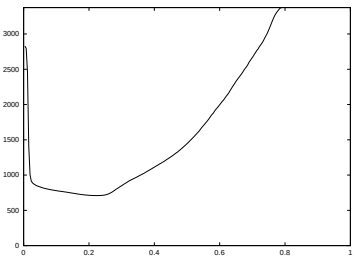

(i) Cost K_p for $M = 2$.

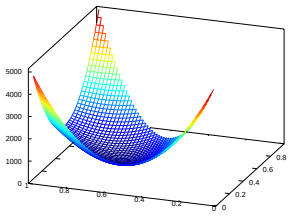

(j) Cost K_p for $M = 3$.

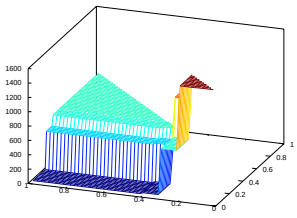

(k) Cost K_p for $M = 3$.

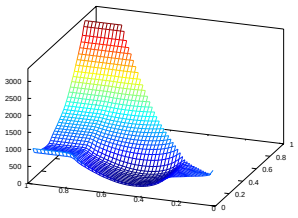

(l) Cost K_p for $M = 3$.

Figure 2: Distribution and cost functions for some sample images.

4 Solving the Optimality System

4.1 Continuity and Differentiability

Let $u : I \to \mathbb{R}$ be an image as usual, p be its distribution function as in Definition 3 and let p be natural. By Equation 9, we already saw that for all intervals J with boundary points $\sigma < \tau$ under the above assumptions we get

$$c_p(J) = c_p\left((\sigma, \tau]\right) = c_p([\sigma, \tau)) = \frac{\int_\sigma^\tau tp'(t)\, dt}{p(\tau) - p(\sigma)}.$$

Let us define $f(\sigma, \tau) = c_p(J)$. Then it is easy to see that f is well-defined for $I^- \leq \sigma < \tau \leq I^+$ because p is strictly monotonic and f is continuously differentiable because p is. The derivatives are given as

$$\frac{\partial f(\sigma,\tau)}{\partial \tau} = \frac{(p(\tau) - p(\sigma))\tau p'(\tau) - p'(\tau)\int_\sigma^\tau tp'(t)\, dt}{(p(\tau) - p(\sigma))^2} = \frac{p'(\tau)}{p(\tau) - p(\sigma)}(\tau - f(\sigma, \tau))$$

and in analogy (numerator and denominator both produce a negative sign)

$$\frac{\partial f(\sigma,\tau)}{\partial \sigma} = \frac{p'(\sigma)}{p(\tau) - p(\sigma)}(\sigma - f(\sigma, \tau)).$$

Lemma 9. *Let p be natural. For $I^- \leq \sigma < \tau \leq I^+$, $f(\sigma, \tau) \in (\sigma, \tau)$. As a consequence, f is continuous at the point (σ, σ).*

Proof. Let $P(t)$ be an anti-derivative of $p(t)$. We use integration by parts and Cauchy's mean value theorem, see [5, p. 273]. By it, there exists $\theta \in (\sigma, \tau)$ such that

$$\begin{aligned} f(\sigma,\tau) &= \frac{\int_\sigma^\tau tp'(t)\, dt}{p(\tau) - p(\sigma)} = \frac{(tp(t) - P(t))|_\sigma^\tau}{p(\tau) - p(\sigma)} \\ &= \frac{p(\theta) + \theta p'(\theta) - p(\theta)}{p'(\theta)} = \theta, \end{aligned}$$

which implies the assertion. Note that all fractions are well-defined because $p'(t) > 0$ is required.

The continuity of $f(\sigma, \sigma)$ follows immediately when remembering that by Definition 6, $f(\sigma, \sigma) = c_p\left((\sigma, \sigma]\right) = \sigma$. □

For the cost function, we get

$$F_p(J) = F_p((\sigma, \tau]) = F_p([\sigma, \tau)) = \int_\sigma^\tau (t - f(\sigma, \tau))^2 p'(t)\, dt;$$

defining $g(\sigma, \tau) = F_p(J)$, g is continuous for all $I^- \leq \sigma \leq \tau \leq I^+$ (taking into account Lemma 9) and also continuously differentiable with respect to σ and τ for $\sigma < \tau$. The derivatives are in this case

$$\frac{\partial g(\sigma,\tau)}{\partial \tau} = (\tau - f(\sigma, \tau))^2 p'(\tau) - 2\frac{\partial f(\sigma,\tau)}{\partial \tau}\int_\sigma^\tau (t - f(\sigma, \tau))p'(t)\, dt.$$

Per Definition 5, the remaining integral vanishes and thus

$$\frac{\partial g(\sigma,\tau)}{\partial \tau} = p'(\tau)(\tau - c_p(J))^2, \quad \frac{\partial g(\sigma,\tau)}{\partial \sigma} = -p'(\sigma)(\sigma - c_p(J))^2. \tag{12}$$

In order to calculate $\nabla K_p(b)$, we have to consider the derivatives $\frac{\partial K_p(b)}{b_i}$ for $i = 1, \ldots, M-1$. For each of those i, the corresponding variable b_i shows up in $K_p(b)$ exactly once as lower and once as upper bound of a $F_p(J)$ summand. For a fixed i, I'll introduce

$$\begin{aligned} c_p^{i+\frac{1}{2}} &= f(b_i, b_{i+1}) = c_p\left((b_i, b_{i+1}]\right) \\ c_p^{i-\frac{1}{2}} &= f(b_{i-1}, b_i) = c_p\left((b_{i-1}, b_i]\right) \end{aligned}$$

for easy notation. (Then $c_p^{i-\frac{1}{2}}$ and $c_p^{i+\frac{1}{2}}$ are the optimal intensities for the segments separated by the boundary b_i in intensity-space.)

Of course, we can use any common technique for finite-dimensional optimization to solve Equation 11, like gradient descent methods. It is also clear from the above analysis that if p is smooth enough, then $K_p(b)$ is even twice continuously differentiable and we can build its Hessian (which will be tridiagonal). Thus, Newton's method can also be applied to find a minimum. However, my calculational results show that Newton's method is very instable numerically in this case because the Hessian can only be found very inexactly via finite differences (numerically, as will be discussed in Section 6, the image u can be processed to give an approximation to p' — but the second derivative is not directly accessible and has to be found from p' via differences which may not give very good results). Other methods also worked for certain cases, although the most efficient are the ones discussed below and summarized in Section 6.

4.2 Optimality Condition

Theorem 10. *If p is natural, there exists a solution b^* in the interior of B satisfying Equation 11. With the notation from above, such a minimizer satisfies*

$$b_i^* = \frac{c_p^{i+\frac{1}{2}} + c_p^{i-\frac{1}{2}}}{2} \tag{13}$$

for all $i = 1, \dots, M-1$.

Proof. We've already seen that $K_p(b)$ is continuous on the whole of B, and because B is compact by Lemma 8, there exists a solution. If b is a solution on the boundary of B, then by Lemma 8 an equality $b_i = b_{i+1}$ holds and the corresponding segmentation has fewer than M segments; by Lemma 3, we can find another segmentation with M segments instead which corresponds to boundaries b^* in the interior of B that is at least as good (and because the original segmentation is a minimizer, is one, too). Thus we can assume that we've got a solution b^* in the interior.

Because $K_p(b)$ is continuously differentiable there, the first order necessary optimality condition for Equation 11 has to be satisfied; with Equation 12 and easy calculation, this implies

$$\frac{\partial K_p(b^*)}{\partial b_i^*} = p'(b_i^*)((b_i^* - c_p^{i-\frac{1}{2}})^2 - (b_i^* - c_p^{i+\frac{1}{2}})^2) = p'(b_i^*)(c_p^{i+\frac{1}{2}} - c_p^{i-\frac{1}{2}})(2b_i^* - c_p^{i+\frac{1}{2}} - c_p^{i-\frac{1}{2}}) \tag{14}$$

and additionally $\frac{\partial K_p(b^*)}{\partial b_i^*} = 0$.

Because $b^* \in B^\circ$, $I^- = b_0 < b_i^* < b_M = I^+$ and thus $p'(b_i^*) > 0$. By Lemma 9, we also get that $c_p^{i+\frac{1}{2}} > c_p^{i-\frac{1}{2}}$ and thus this condition is equivalent to $2b_i^* - c_p^{i+\frac{1}{2}} - c_p^{i-\frac{1}{2}} = 0$ which implies the assertion. □

Note the similarity between $\frac{\partial K_p(b)}{\partial b_i}$ (in the first equality of Equation 14) and the topological derivative in Equation 3. But because a change of b_i does not hand over a small ball of the image domain between segments but instead all points with the intensity b_i, the additional weighting factor $p'(b_i)$ has to be there.

In the rest of this subsection, I want to illustrate the optimality system Equation 13 and the minimization in Equation 11 with a simple example. Consider the image of Figure 2a, which can be characterized by its distribution function

$$p(x) = \begin{cases} 0 & x \le 0 \\ x & 0 \le x \le 1 \\ 1 & 1 \le x \end{cases} .$$

It is continuously differentiable and $p'(x) = 1 > 0$ for $I^- = 0 < x < 1 = I^+$, thus natural. Let $M > 1$ be given, and we try to find the best segmentation of this image. Given two boundaries $0 < \sigma < \tau < 1$, the corresponding segment's intensity is

$$c_p\left((\sigma, \tau]\right) = \frac{\int_\sigma^\tau t p'(t)\, dt}{p(\tau) - p(\sigma)} = \frac{\int_\sigma^\tau t\, dt}{\tau - \sigma} = \frac{\sigma + \tau}{2}.$$

Then for $i = 1, \dots, M-1$, the boundaries b_i must satisfy the optimality condition of Theorem 10:

$$2b_i = c_p^{i+\frac{1}{2}} + c_p^{i-\frac{1}{2}} = \frac{b_{i+1} + b_i + b_i + b_{i-1}}{2} \;\Leftrightarrow\; b_i = \frac{b_{i+1} + b_{i-1}}{2}$$

which is equivalent to the system of linear equations

$$\begin{aligned} b_1 &= \frac{1}{2}(b_2 + b_0) = \frac{1}{2}b_2 \\ b_2 &= \frac{1}{2}(b_3 + b_1) \\ &\vdots \\ b_{M-1} &= \frac{1}{2}(b_M + b_{M-2}) = \frac{1}{2}(1 + b_{M-2}). \end{aligned}$$

The unique solution to this system is $b_i = \frac{i}{M}$ for $i = 1, \ldots, M-1$ and thus it also has to be the solution guaranteed by Theorem 10. In fact, this is also quite reasonable, as it means that the intensity-space is divided into equal segments which clearly is a good choice for the example image.

4.3 Fixed-Point Iteration

Definition 7. For p natural and with the notation of above, define a set of maps $\Psi_i : B \to \mathbb{R}^{M-1}$ for $i = 1, \ldots, M-1$ such that

$$\Psi_i(b) = \left(b_1, \ldots, b_{i-1}, \frac{c_p^{i+\frac{1}{2}} + c_p^{i-\frac{1}{2}}}{2}, b_{i+1}, \ldots, b_{M-1} \right),$$

and also $\Phi : B \to \mathbb{R}^{M-1}$ by

$$\Phi(b) = \left(\frac{c_p^{i+\frac{1}{2}} + c_p^{i-\frac{1}{2}}}{2} \right)_{i=1}^{M-1}.$$

Lemma 11. *For $b \in B$ and $i = 1, \ldots, M-1$, it holds that $\Psi_i(b), \Phi(b) \in B$; i.e., B is invariant under those maps (and thus they are functions $B \to B$). Similarly, for $b \in B^\circ$ and $i = 1, \ldots, M-1$, we have $\Psi_i(b), \Phi(b) \in B^\circ$.*

Proof. Let $i = 1, \ldots, M-1$. Define $\overline{b}_i = \frac{c_p^{i+\frac{1}{2}} + c_p^{i-\frac{1}{2}}}{2}$ (i.e., $\overline{b} = \Phi(b)$), $c_p^{i+\frac{3}{2}} = c_p\left((b_{i+1}, b_{i+2}]\right)$ and $c_p^{i-\frac{3}{2}} = c_p\left((b_{i-2}, b_{i-1}]\right)$. Then taking Lemma 9 into account:

$$\overline{b}_i = \frac{c_p^{i+\frac{1}{2}} + c_p^{i-\frac{1}{2}}}{2} \geq \frac{b_i + b_{i-1}}{2} \geq b_{i-1}.$$

For $\overline{b} \in B^\circ$, even strict inequality holds. Similarly one obtains $\overline{b}_i \leq b_{i+1}$ and strict inequality in the interior of B. Also

$$\overline{b}_i \geq \frac{b_i + b_{i-1}}{2} \geq \frac{c_p^{i-\frac{1}{2}} + c_p^{i-\frac{3}{2}}}{2} = \overline{b}_{i-1}$$

with strict inequality for $\overline{b} \in B^\circ$. By analogues, $\overline{b}_i \leq \overline{b}_{i+1}$. From this, the assertion easily follows. □

Theorem 12. *Let p be natural and define $\Phi : B \to B$, $\Psi_i : B \to B$ as in Definition 7. Then $b \in B$ is a fixed-point of Φ if and only if it is a common fixed-point of all Ψ_i. There exists $b^* \in B^\circ$ satisfying Equation 11, which is such a fixed-point.*

Proof. The functions are well-defined because of Lemma 11 and the equivalence is clear per definition. Existence follows from Theorem 10. □

Thus we can attempt to find an optimal segmentation via Equation 11 by doing a fixed-point iteration either with Φ directly or for instance with

$$\Psi = \Psi_{M-1} \circ \cdots \circ \Psi_1$$

in a "Gauß-Seidel" like manner.

Lemma 13. *Let p be natural and consider $\Phi : B \to B$ and $\Psi_i : B \to B$ as in Definition 7. Then for every $b \in B^\circ$, both $\Phi(b) - b$ and $\Psi_i(b) - b$ are descent directions for $K_p(b)$ or zero.*

Proof. Let $i = 1, \ldots, M-1$ and $b \in B^\circ$ be given, and set $d = \Psi_i(b) - b$; suppose $d \neq 0$. We have to show $d \cdot \nabla K_p(b) < 0$ in order to prove that d is a descent direction. The proof for $\Phi(b) - b$ goes the same.

Clearly, $d_i = \frac{c_p^{i+\frac{1}{2}} + c_p^{i-\frac{1}{2}}}{2} - b_i$ and $d_j = 0$ for $j \neq i$. Thus (using Equation 14)

$$d \cdot \nabla K_p(b) = d_i \frac{\partial K_p(b)}{\partial b_i} = \left(\frac{c_p^{i+\frac{1}{2}} + c_p^{i-\frac{1}{2}}}{2} - b_i \right) \cdot p'(b_i)(c_p^{i+\frac{1}{2}} - c_p^{i-\frac{1}{2}})(2b_i - c_p^{i+\frac{1}{2}} - c_p^{i-\frac{1}{2}}).$$

Because p is natural and $b \in B^\circ$, $p'(b_i)(c_p^{i+\frac{1}{2}} - c_p^{i-\frac{1}{2}}) > 0$. As $d \neq 0$, we know that $b_i \neq \frac{c_p^{i+\frac{1}{2}} + c_p^{i-\frac{1}{2}}}{2}$ must hold. It remains to observe that

$$0 > \left(\frac{c_p^{i+\frac{1}{2}} + c_p^{i-\frac{1}{2}}}{2} - b_i \right) \cdot (2b_i - c_p^{i+\frac{1}{2}} - c_p^{i-\frac{1}{2}}) = -2 \left(\frac{c_p^{i+\frac{1}{2}} + c_p^{i-\frac{1}{2}}}{2} - b_i \right)^2 .$$

□

While I unfortunately can not present a full proof of convergence of the fixed-point iterations, Lemma 13 at least gives some justification to them as optimization strategies. In principle, instead of doing the full iteration, those descent directions could be used together with a suitable line-search algorithm in order to improve convergence should this be necessary in practice. An additional result is as follows:

Theorem 14. *For fixed segment-intensities $c_1 < c_2 < \ldots < c_M$, the segmentation corresponding to the boundaries given by $b_0 = I^-$, $b_M = I^+$ and $b_i = \frac{c_i + c_{i+1}}{2}$ for $i = 1, \ldots, M-1$ has minimal relative error. As a consequence, $K_p(\Phi(b)) \leq K_p(b)$ for all $b \in B$. Equality may only hold if $\Phi(b)$ is a fixed-point of Φ.*

Proof. By the proof of Lemma 4, for fixed intensities the domains B_i per Equation 6 minimize the relative error. To express Equation 6 in terms of the boundaries, I will show that $B_1 = u^{-1}([I^-, b_1])$ and $B_i = u^{-1}((b_{i-1}, b_i])$ for $i = 2, \ldots, M$. Because the intensities are sorted, the condition

$$\forall j < i : \ |u(x) - c_i| < |u(x) - c_j| \ \text{ and } \forall j > i : \ |u(x) - c_i| \leq |u(x) - c_j|$$

of Equation 6 is equivalent to

$$|u(x) - c_i| < |u(x) - c_{i-1}| \ \text{ and } \ |u(x) - c_i| \leq |u(x) - c_{i+1}| .$$

This, however, is fulfilled if and only if

$$b_{i-1} = \frac{c_i + c_{i-1}}{2} < u(x) \leq \frac{c_i + c_{i+1}}{2} = b_i,$$

which is equivalent to $x \in u^{-1}((b_{i-1}, b_i])$ as was to show.

If c_i are the intensities given by Equation 2 for the segmentation corresponding to $b \in B$, then the optimal boundaries as by the first part of this proof are $\Phi(b)$. $K_p(\Phi(b))$ is by Theorem 2 smaller than the cost of the segmentation with intensities c_i and boundaries $\Phi(b)$, which in turn is not larger than $K_p(b)$ by the first part of this theorem. Thus $K_p(\Phi(b)) \leq K_p(b)$. Because of the uniqueness in Theorem 2, equality can only hold if all c_i are already the optimal intensities for the boundaries $\Phi(b)$, but then $\Phi(\Phi(b)) = \Phi(b)$ because Φ depends only on the optimal intensities of a segmentation and those are the same for b and $\Phi(b)$. □

The result of strict decrease if not already at a fixed-point excludes the possibility that a limit-cycle (such that $b = \Phi^k(b)$ for some $k > 2$) exists for the fixed-point iteration with Φ. However, this not necessarily implies convergence towards a fixed-point as the trajectory of some $b \in B$ may have multiple accumulation points with only asymptotic convergence towards them.

Note that Theorem 14 and its proof also makes clear that the fixed-point iteration with Φ is nothing else than application of the well-known k-means clustering algorithm (see [9, p. 285f]) to the problem of image segmentation: There, an iteration with alternating steps is performed. First, for given domains the "optimal" mean values are calculated in the same way as motivated by Theorem 2 (which is already implicitly included in my practice of describing segments by their boundaries). Second, for given mean values, the items to be clustered are assigned to "optimal" domains by a Voronoi tessellation in the image range space based on the current mean values; but in the case of image segmentation, this is nothing else than transforming b into $\Phi(b)$ as we have just seen. This application of k-means to image segmentation is an adaption to an infinite set of items, though, while the classical algorithm is usually formulated for a finite set. So this work can be seen as a measure theoretic derivation of the k-means clustering algorithm applied to image segmentation.

4.4 Sequential Construction of the Fixed-Point

When an intensity bound $b_1 \in I$ is given and Equation 13 should be satisfied, we can successively calculate $b_2, \ldots, b_{M-1}$ from this condition. Of course, $b_M = I^+$ does not in general also satisfy the relevant equation (only if the b_1 we started with actually belongs to a solution point). I'll now formalize this idea to give a construction of the solution boundaries $b \in B$.

Lemma 15. *Let p be natural, $D = \{(\sigma, \tau) \mid \sigma \in I, \tau \in [\sigma, I^+]\}$ and define $f : D \to I$ by $f(\sigma, \tau) = c_p((\sigma, \tau])$. Let us further for fixed $\sigma, \tau \in I$ define $f_\sigma : [\sigma, I^+] \to I, \tau \mapsto f(\sigma, \tau)$ and $\overline{f}_\tau : [I^-, \tau] \to I, \sigma \mapsto f(\sigma, \tau)$.*

Then f, f_σ and $\overline{f}_\tau$ are continuous, f_σ and $\overline{f}_\tau$ are strictly increasing. Their images are compact intervals and on these, f_σ and $\overline{f}_\tau$ are continuously invertible. If β and g are continuous functions, the solution t to

$$f(\beta(\tau), t) = g(\tau) \tag{15}$$

depends continuously on τ.

Proof. Continuity of f follows from Lemma 9, as does the continuity of f_σ and $\overline{f}_\tau$. Again because of Lemma 9, $f_\sigma(\sigma) < f_\sigma(\tau)$ for all $\tau \in (\sigma, I^+]$. Additionally we find

$$f'_\sigma(\tau) = \frac{\partial f(\sigma, \tau)}{\partial \tau} = \frac{p'(\tau)}{p(\tau) - p(\sigma)}(\tau - f(\sigma, \tau))$$

which is strictly positive for $\tau > \sigma$ because of $f(\sigma, \tau) \in (\sigma, \tau)$. Similarly it follows that also $\overline{f}_\tau$ is strictly increasing.

Because f_σ and $\overline{f}_\tau$ are continuous and defined on a compact interval, their images are also compact intervals by [5, p. 235]. They are injective because they are strictly increasing, and thus on their image continuously invertible ([5, p. 233]).

Now, let $(\tau_n) \to \tau$ be a convergent sequence and $(t_n), t$ be given such that Equation 15 holds for all pairs (τ_n, t_n) and also for (τ, t). If (t_n) converges to some s, then we can take the limit $n \to \infty$ in Equation 15 and get $f(\beta(\tau), s) = g(\tau)$. As $f_{\beta(\tau)}$ is injective, $t = s$ follows and thus $(t_n) \to t$. Because $(t_n) \subset I$, it is bounded; for each convergent sub-sequence, we get by the argument above that its limit must be t. Thus $(t_n) \to t$. □

Lemma 16. *Let p be natural and $M \geq 2$. Then there exist $\hat{\theta} \in I$ and functions β_i, $i = 1, \ldots, M-1$, such that:*

(a) $\beta_i : [I^-, \hat{\theta}] \to I$ for $i = 0, \ldots, M-1$,

(b) all β_i are continuous,

(c) $\beta_0(\theta) = I^-$, $\beta_1(\theta) = \theta$,

(d) $\forall \theta \in [I^-, \hat{\theta}] : \beta_0(\theta) \leq \beta_1(\theta) \leq \cdots \leq \beta_{M-1}(\theta)$,

(e) $\beta_{M-1}(I^-) = I^-$ and $\beta_{M-1}(\hat{\theta}) = I^+$,

(f) for $i = 1, \ldots, M-2$ and all $\theta \in [I^-, \hat{\theta}]$: $2\beta_i(\theta) = f(\beta_i(\theta) + \beta_{i+1}(\theta)) + f(\beta_{i-1}(\theta), \beta_i(\theta))$.

(g) Let b_i, $i = 0, \ldots, M$, be given with $b_0 = I^-$ and $b_M = I^+$. Then $b_i = \frac{c_p^{i+\frac{1}{2}} + c_p^{i-\frac{1}{2}}}{2}$ holds for $i = 1, \ldots, M-1$ if and only if there exists a unique $\theta^* \in [I^-, \hat{\theta}]$ such that $b_i = \beta_i(\theta^*)$ for all i.

Proof. We'll show this by induction with respect to M. In the case $M = 2$, we take $\hat{\theta} = I^+$ and β_0, β_1 according to (c). Then the conditions (a), (b), (d) and (e) hold trivially. Condition (f) does not apply because the range of i is empty in this case. Finally, condition (g) is considered at the end of the proof for a general M.

Now assume the assertions (a)–(f) hold for $M \geq 2$. Let $\beta_0, \ldots, \beta_{M-1}$ be the functions already satisfying them for some θ' in place of $\hat{\theta}$. We have to define β_M and a new $\hat{\theta}$. Let $f(\sigma, \tau) = c_p((\sigma, \tau])$ be as in Lemma 15 and define $x(\sigma, \tau) = \tau + (\tau - f(\sigma, \tau))$. Then clearly, both f and x are continuous and $f(\sigma, \tau) \in [\sigma, \tau]$ as well as $x(\sigma, \tau) \geq \tau$ holds.

Define functions $g(\theta) = x(\beta_{M-2}(\theta), \beta_{M-1}(\theta))$ and $m(\theta) = f(\beta_{M-1}(\theta), I^+)$. As compositions of continuous functions, again both g and m are continuous themselves. Set $D = \{\theta \in [I^-, \theta'] \mid g(\theta) \leq m(\theta)\}$.

Note that $D \neq \emptyset$, since $g(I^-) = I^-$ and $m(I^-) = f(I^-, I^+) \in (I^-, I^+)$ implies $I^- \in D$. Because of $g(I^-) < m(I^-)$, it follows from the continuity of these functions that there is an $\epsilon > 0$ such that $g(\theta) < m(\theta)$ holds for all $\theta \in [I^-, I^- + \epsilon]$. Thus if we define $\hat{\theta} = \sup D$, it follows that $I^+ \geq \hat{\theta} \geq I^- + \epsilon > I^-$. Also, since $I^+ \geq f(\beta_{M-2}(\theta'), I^+)$ implies

$$g(\theta') = 2I^+ - f(\beta_{M-2}(\theta'), I^+) \geq I^+ = f(I^+, I^+) = m(\theta'),$$

it follows that $\hat{\theta} \leq \theta'$. Finally note that a strict inequality $g(\hat{\theta}) < m(\hat{\theta})$ or $g(\hat{\theta}) > m(\hat{\theta})$ would be preserved in a neighbourhood of $\hat{\theta}$ due to continuity of these functions. Since such a strict inequality would violate the definition of $\hat{\theta}$, it follows that $g(\hat{\theta}) = m(\hat{\theta})$ holds.

By condition (a), $\beta_{M-1}(\theta) \in I$ holds for all $\theta \in [I^-, \theta']$, so since $\hat{\theta} \leq \theta'$ it follows from Lemma 15 that for each $\theta \in [I^-, \hat{\theta}]$ the function $f_{\beta_{M-1}(\theta)}$ is defined on $[\beta_{M-1}(\theta), I^+]$ and it is invertible on its range. Since $f_{\beta_{M-1}(\theta)}$ is increasing and $f_{\beta_{M-1}(\theta)}(\beta_{M-1}(\theta)) = \beta_{M-1}(\theta)$ and $f_{\beta_{M-1}(\theta)}(I^+) = m(\theta)$ holds, it follows that the range of $f_{\beta_{M-1}(\theta)}$ is $[\beta_{M-1}(\theta), m(\theta)]$. From condition (d) and $f(\beta_{M-2}(\theta), \beta_{M-1}(\theta)) \leq \beta_{M-1}(\theta)$ it follows that

$$\beta_{M-1}(\theta) \leq 2\beta_{M-1}(\theta) - f(\beta_{M-2}(\theta), \beta_{M-1}(\theta)) = g(\theta)$$

for all $\theta \in [I^-, \theta']$. Also, $g(\theta) \leq m(\theta)$ holds for all $\theta \in [I^-, \hat{\theta}]$ because of the definition of $\hat{\theta}$. Thus, $g(\theta)$ is in the range of $f_{\beta_{M-1}(\theta)}$ for all $\theta \in [I^-, \hat{\theta}]$. Hence, the function $\beta_M(\theta)$ may be defined according to $f_{\beta_{M-1}(\theta)}(\beta_M(\theta)) = g(\theta)$ or as the unique solution to

$$f(\beta_{M-1}(\theta), \beta_M(\theta)) = g(\theta)$$

for each $\theta \in [I^-, \hat{\theta}]$ (see Lemma 15 and Equation 15).

Since the solution $\tau = \beta_M(\theta)$ to $f(\beta_{M-1}(\theta), \tau) = g(\theta)$ necessarily lies in the definition range of $f_{\beta_{M-1}(\theta)}$, the inequality $I^- \leq \beta_{M-1}(\theta) \leq \beta_M(\theta) \leq I^+$ holds for all $\theta \in [I^-, \hat{\theta}]$. Thus, (a) is established for β_M. The same inequality implies also condition (d). By Lemma 15, β_M is continuous which gives (b). Because $\beta_{M-1}(I^-) = I^-$ and thus

$$f(\beta_{M-1}(I^-), I^-) = f(I^-, I^-) = I^- = x(I^-, I^-) = g(I^-),$$

it follows with Lemma 15 that $\beta_M(I^-) = I^-$. Similarly, by $f(\beta_{M-1}(\hat{\theta}), I^+) = m(\hat{\theta}) = g(\hat{\theta})$ we get $\beta_M(\hat{\theta}) = I^+$ and thus condition (e). Finally, condition (f) follows for β_M from $f(\beta_{M-1}(\theta), \beta_M(\theta)) = g(\theta)$.

It remains now to prove the claim (g). First, suppose $b_i = \frac{c_p^{i+\frac{1}{2}} + c_p^{i-\frac{1}{2}}}{2}$ holds for $i = 1, \ldots, M-1$. Then choose $\theta^* = b_1$ and note that $\beta_1(\theta^*) = b_1$. Assume now inductively for $i \geq 1$ that $b_j = \beta_j(\theta^*)$ holds for $j = 1, \ldots, i$. By condition (f),

$$f(b_i, b_{i+1}) = x(b_{i-1}, b_i) = x(\beta_{i-1}(\theta^*), \beta_i(\theta^*)) = f(\beta_i(\theta^*), \beta_{i+1}(\theta^*)) = f(b_i, \beta^*_{i+1}).$$

Thus by Lemma 15, $b_{i+1} = \beta_{i+1}(\theta^*)$. If $\tilde{\theta}$ were any other value satisfying $b_i = \beta_i(\theta)$ for $i = 1, \ldots, M-1$, then $\tilde{\theta} = \beta_1(\tilde{\theta}) = b_1 = \theta^*$. Thus, θ^* is unique.

Now on the other hand, assume there is a unique $\theta^* \in [I^-, \hat{\theta}]$ such that $b_i = \beta_i(\theta^*)$ for $i = 1, \ldots, M-1$. Then by condition (f),

$$b_i = \beta_i(\theta^*) = \frac{1}{2}\left(f(\beta_i(\theta^*), \beta_{i+1}(\theta^*) + f(\beta_{i-1}(\theta^*), \beta_i(\theta^*))\right) = \frac{1}{2}\left(f(b_i, b_{i+1}) + f(b_{i-1}, b_i)\right) = \frac{c_p^{i+\frac{1}{2}} + c_p^{i-\frac{1}{2}}}{2}.$$

□

Theorem 17. *Let p be natural and the definitions from Lemma 16 apply. Let $b = (b_1, \ldots, b_{M-1}) \in B$ be any solution to the problem in Equation 11, whose existence is guaranteed by Theorem 10. Then there exists a unique $\theta^* \in (I^-, \hat{\theta})$ such that $b_i = \beta_i(\theta^*)$ for $i = 1, \ldots, M-1$.*

Proof. According to Theorem 10, a solution b to the problem of Equation 11 is characterized by Equation 13, and thus b is a fixed-point for Φ. According to condition (g) in Lemma 16, there exists a unique $\theta^* \in [I^-, \hat{\theta}]$ such that $b_i = \beta_i(\theta^*)$ for all $i = 1, \ldots, M-1$. It remains to show that $\theta^* \in (I^-, \hat{\theta})$.

For this, define the map $\delta : [I^-, \hat{\theta}] \to \mathbb{R}$ by

$$\delta(\theta) = \beta_{M-1}(\theta) - \frac{f(\beta_{M-1}(\theta), I^+) + f(\beta_{M-2}(\theta), \beta_{M-1}(\theta))}{2}.$$

Then δ is clearly continuous and the point $b = (b_1, \ldots, b_{M-1}) = (\beta_1(\theta^*), \ldots, \beta_{M-1}(\theta^*)) \in B$ is a fixed-point of Φ if and only if $\delta(\theta^*) = 0$. It can not be that $\theta^* = I^-$ holds, since

$$\delta(I^-) = I^- - \frac{f(I^-, I^+) + f(I^-, I^-)}{2} = \frac{I^- - f(I^-, I^+)}{2} < 0.$$

On the other hand,

$$\delta(\hat{\theta}) = I^+ - \frac{f(I^+, I^+) + f(\beta_{M-2}(\hat{\theta}), I^+)}{2} = \frac{I^+ - f(\beta_{M-2}(\hat{\theta}), I^+)}{2} \geq 0.$$

That $\theta^* = \hat{\theta}$ can not hold is established as follows: Assume that

$$0 = \delta(\hat{\theta}) = \frac{I^+ - f(\beta_{M-2}(\hat{\theta}), I^+)}{2}.$$

Then necessarily $\beta_{M-2}(\hat{\theta}) = \beta_{M-1}(\hat{\theta}) = I^+$. Let $k \leq M-2$ be such that $\beta_{k-1}(\hat{\theta}) < \beta_k(\hat{\theta}) = I^+$; such a k exists because $\beta_0(\hat{\theta}) = I^- < I^+$. But then according to Lemma 16,

$$\begin{aligned} I^+ &= \beta_k(\hat{\theta}) = \frac{f(\beta_k(\hat{\theta}), \beta_{k+1}(\hat{\theta})) + f(\beta_{k-1}(\hat{\theta}), \beta_k(\hat{\theta}))}{2} \\ &= \frac{I^+ + f(\beta_{k-1}(\hat{\theta}), I^+)}{2} < I^+, \end{aligned}$$

which is a contradiction. Thus $\delta(\hat{\theta}) > 0$ and in particular $\delta(\hat{\theta}) \neq 0$, which implies the claim. □

Note that because $\delta(I^-) < 0$ and $\delta(\hat{\theta}) > 0$ in the proof of Theorem 17, at least one $\theta^* \in (I^-, \hat{\theta})$ with $\delta(\theta^*)$, thus corresponding to a fixed-point, can be constructed by the intermediate value theorem (see [5, p. 234f]). Additionally, also the construction of the inverse function in Lemma 15 and the β_i's in Lemma 16 are all nearly explicit. By methods like interval bisection, this sequential construction of a fixed-point can be actually done in practice numerically and thus used as a way to find a possible best segmentation. However, this is clearly "asymmetric" in nature (as we start at the lower boundaries and successively construct the upper ones) and also susceptible to rounding errors and unprecise results due to numerical integration in certain cases — but it may be used to generate some initial segmentation which is used as starting-point for a fixed-point iteration as in Definition 7. This will be discussed in more detail in Section 6.

4.5 Non-Unique Fixed-Points

Unfortunately, the fixed-point of Theorem 12 can not be guaranteed to be unique. In this final subsection, I will give an example where this is illustrated.

Consider again the sequential construction done in the proof of Lemma 16: Given two boundaries b_{i-2} and b_{i-1}, we wanted to construct the next one b_i such that Equation 13 holds. For this, we defined a function $x(\sigma, \tau) = \tau + (\tau - c_p((\sigma, \tau])))$ which determines, according to the optimality system, the required segment-intensity of b_{i-1} and b_i. This value must match the actual segment-intensity according to $c_p((\sigma, \tau]) = x(\sigma, \tau)$. The construction is unique if x is strictly increasing (i.e., injective). However, this needs not be the case, because

$$\frac{\partial x(\sigma, \tau)}{\partial \tau} = 2 - \frac{\partial c_p((\sigma, \tau])}{\partial \tau} = 2 - \frac{p'(\tau)}{p(\tau) - p(\sigma)}(\tau - c_p((\sigma, \tau])))$$

may be positive or negative. It may well be negative especially if $p'(\tau)$ is large, i.e., p steep around τ.

It is possibly surprising that $x(\sigma, \tau)$ may actually decrease when increasing τ. But one may consider that, as a function of τ, $x(\sigma, \tau)$ is the "mirror image" of $c_p((\sigma, \tau])$ in the following sense: If p is very steep around τ, then increasing τ can increase $c_p((\sigma, \tau])$ strongly, because a large area of intensity near τ is included in the average-value calculation and thus the result is shifted towards τ. This increase in $c_p((\sigma, \tau])$ may be much more rapid than the increase in τ, and because of the term $(\tau - c_p((\sigma, \tau])))$ above, $x(\sigma, \tau)$ may actually decrease.

For the promised example where this actually happens, consider intensities in $I = [0, 1]$. Define for parameters $\mu = \frac{1}{2}$ and $\delta = 1000$ the functions

$$\begin{aligned} f(t) &= \frac{t}{\sqrt{t^2 + 1}} \\ g(t) &= f(\delta t) + t \end{aligned}$$

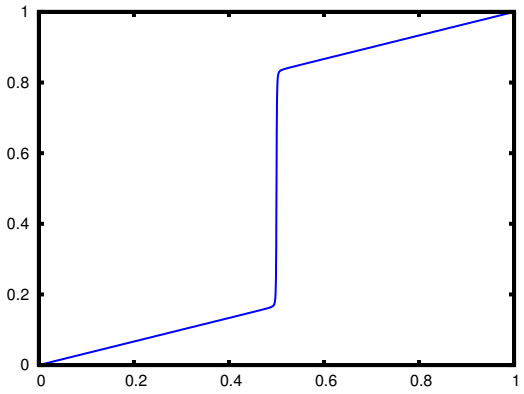

(a) Distribution p.

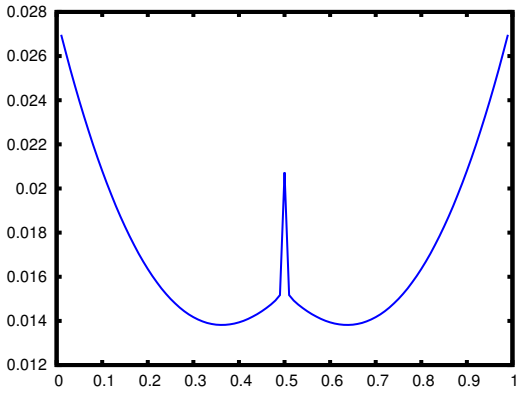

(b) Cost K_p.

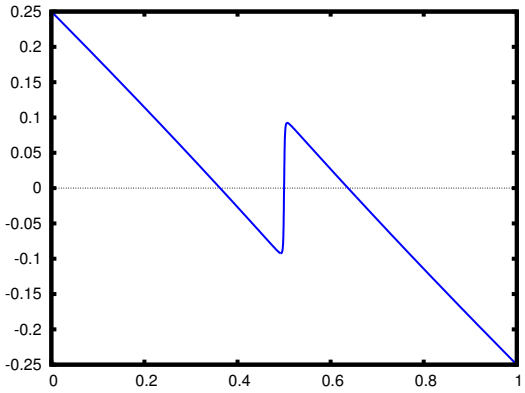

(c) $\Phi(b) - b$ for fixed-points.

Figure 3: Example for non-unique fixed-point.

and with those the distribution function

$$p(t) = \frac{g(\mu) - g(\mu - t)}{g(\mu) - g(\mu - 1)}. \tag{16}$$

Then it is easy to see that p as defined in Equation 16 satisfies $p(0) = 0$, $p(1) = 1$, is strictly increasing because f is strictly increasing, and p is continuously differentiable on I. Thus it actually is a natural distribution function.

I will not give detailed calculations for the following results, but it is possible to symbolically calculate $c_p((\sigma, \tau])$ as well as $\Phi(b)$ for $M = 2$ and p as in Equation 16. The calculations were performed using the Computer Algebra System Maxima 5.17.1, see [2]. This p is shown in Figure 3a. Figure 3b shows the corresponding cost $K_p(b)$, and in Figure 3c the function $\Phi(b) - b$ is plotted. It has three zeros, all of which are fixed-points. Those fixed-points correspond to the local optima of the cost, which include two minima and one maximum. So in this case, there is no unique fixed-point, and one of the fixed-points even corresponds to a local maximum rather than minimum.

5 Adding Noise to the Image

Images that are measured — for instance, ordinary photographs or magnetic resonance images — can never really exactly represent the original object, but because of inexactness and disturbance in the measurement process have noise added to them. In this section, I will consider the effect this has on the segmentation method and analysis done above, most prominently in Section 4.

While noise is usually regarded as a problem or at least nuisance, we'll see that in this context it can have a rather positive impact as it ensures under certain reasonable conditions that p (as per Definition 3) of the noisy image is natural, even if it would not be so for the original image.

Definition 8. Let $u : \Omega \to I$ be an image, let p_0 be the distribution function defined in Definition 3 for u and let $(\Omega, \mathcal{F}, \pi)$ be the probability space introduced there. Further, assume that n is a real random variable such that u and n are independent and $f_n : \mathbb{R} \to \mathbb{R}$ is the probability density function of n. f_n shall be continuously differentiable and ${f_n}^{-1}((0,\infty)) = (I_n^-, I_n^+)$. That is, the support of n shall be the compact interval $[I_n^-, I_n^+]$.

Then for some noise-level $\nu > 0$, $\tilde{u} = u + \nu n$ is another real random variable; it is the image u with noise added. Let p_ν be the corresponding distribution function.

Lemma 18. *p_ν has "compact support", meaning that $p_\nu(x) = 0$ for all $x \leq I^- + \nu I_n^-$ and $p_\nu(x) = 1$ for all $x \geq I^+ + \nu I_n^+$. p_ν is given by*

$$p_\nu(x) = \frac{1}{\nu} \int_{-\infty}^{\infty} p_0(u) f_n\left(\frac{x-u}{\nu}\right)\, du. \tag{17}$$

Proof. I'll first show that Equation 17 holds:

$$\begin{aligned} p_\nu(x) &= P\left(u + \nu n \leq x\right) = \int_{-\infty}^{\infty} P\left(u \leq x - \nu\xi\right) f_n(\xi)\, d\xi \\ &= \int_{-\infty}^{\infty} p_0(x - \nu\xi) f_n(\xi)\, d\xi = \frac{1}{\nu} \int_{-\infty}^{\infty} p_0(u) f_n\left(\frac{x-u}{\nu}\right)\, du \end{aligned}$$

Now, let $x \leq I^- + \nu I_n^-$. Then clearly $\frac{x-u}{\nu} \leq \frac{I^- - u}{\nu} + I_n^-$. For $u < I^-$, we have that $p_0(u) = 0$; but for $u \geq I^-$, it follows that $\frac{x-u}{\nu} \leq I_n^-$ and thus $f_n\left(\frac{x-u}{\nu}\right) = 0$, so that by the formula above $p_\nu(x) = 0$. Let $x \geq I^+ + \nu I_n^+$. Then as before $\frac{x-u}{\nu} \geq \frac{I^+ - u}{\nu} + I_n^+$. If $u \leq I^+$, then $\frac{x-u}{\nu} \geq I_n^+$ and thus $f_n\left(\frac{x-u}{\nu}\right) = 0$. So

$$\begin{aligned} p_\nu(x) &= \frac{1}{\nu} \int_{I^+}^{\infty} p_0(u) f_n\left(\frac{x-u}{\nu}\right)\, du = \frac{1}{\nu} \int_{I^+}^{\infty} f_n\left(\frac{x-u}{\nu}\right)\, du \\ &= -\int_{\frac{x-I^+}{\nu}}^{-\infty} f_n(\xi)\, d\xi \geq \int_{-\infty}^{I_n^+} f_n(\xi)\, d\xi = 1, \end{aligned}$$

because $\frac{x-I^+}{\nu} \geq I_n^+$ and f_n is a density function. $p_\nu(x) \leq 1$ because it is a cumulative distribution function, thus $p_\nu(x) = 1$ as was to show. □

Theorem 19. *p_ν is continuously differentiable. Let $d = \nu(I_n^+ - I_n^-)$. If for all $x \in (I^-, I^+)$ we have $p_0(x) > p_0(x - \frac{d}{2})$ (which means that the "gaps" in intensity-space where p_0 is constant are smaller than the noise's bandwidth), then $p_\nu'(x) > 0$ for all x such that $0 < p_\nu(x) < 1$. This essentially means that p_ν is natural in this case.*

Proof. Because f_n is continuously differentiable, it is evident by Lemma 18 and Equation 17 that p_ν is continuously differentiable.

So assume that the gap inequality holds for p_0 and let x be given such that $0 < p_\nu(x) < 1$. Assume for now that we have $\sigma < \tau$ such that $p_0(\tau) > p_0(\sigma)$ and $f_n\left(\frac{x-u}{\nu}\right) > 0$ for all $u \in [\sigma, \tau]$. As f_n is continuous and $[\sigma, \tau]$ compact, this actually means that f_n is bounded away from zero, thus $\inf_{u\in[\sigma,\tau]} f_n\left(\frac{x-u}{\nu}\right) > 0$. Then:

$$\begin{aligned} p_\nu'(x) &= \frac{1}{\nu^2} \int_{-\infty}^{\infty} p_0(u) f_n'\left(\frac{x-u}{\nu}\right)\, du = \frac{1}{\nu} \int_{-\infty}^{\infty} f_n\left(\frac{x-u}{\nu}\right)\, dp_0(u) \\ &\geq \frac{1}{\nu} \left(\inf_{u\in[\sigma,\tau]} f_n\left(\frac{x-u}{\nu}\right)\right) \int_{(\sigma,\tau]} dp_0(u) \\ &= \frac{1}{\nu} \left(\inf_{u\in[\sigma,\tau]} f_n\left(\frac{x-u}{\nu}\right)\right) (p_0(\tau) - p_0(\sigma)) > 0 \end{aligned}$$

So in order to complete the proof, we have to find σ and τ satisfying the assumptions made above.

If for all u with $f_n\left(\frac{x-u}{\nu}\right) > 0$ we have $p_0(u) = 0$, then clearly $p_\nu(x) = 0$. On the other hand, if for all of them $p_0(u) = 1$, then as in the proof of Lemma 18 we get $p_\nu(x) = 1$. Recall that x was chosen such that $0 < p_\nu(x) < 1$, thus by the argument above, on the set of u's with $f\left(\frac{x-u}{\nu}\right) > 0$, there exist u's with $p_0(u) > 0$ and there exist u's with $p_0(u) < 1$. But suppose that there is no such u with $0 < p_0(u) < 1$, then for all of them $p_0(u) \in \{0, 1\}$. This however is a contradiction to Definition 1 and thus there exists a u such that $f_n\left(\frac{x-u}{\nu}\right) > 0$ and also $0 < p_0(u) < 1$. Let $s = x - u - \nu I_n^-$, then $s > 0$ because $\frac{x-u}{\nu} > I_n^-$.

If $p_0(u) < p_0\left(u + \frac{s}{2}\right)$, then $\sigma = u$ and $\tau = u + \frac{s}{2}$ satisfy the requirements: $f_n\left(\frac{x-u}{\nu}\right) > 0$ holds per construction, and

$$f_n\left(\frac{x-\tau}{\nu}\right) = f_n\left(\frac{x-u-\frac{s}{2}}{\nu}\right) = f_n\left(\frac{1}{2}\frac{x-u}{\nu} + \frac{I_n^-}{2}\right).$$

Because $\frac{x-u}{\nu} > I_n^-$, the argument is surely greater than I_n^-. On the other hand, $\frac{x-u}{\nu} < I_n^+$ and thus the argument is also less than $\frac{I_n^- + I_n^+}{2} < I_n^+$, so that $f_n\left(\frac{x-b}{\nu}\right) > 0$. Because the support of f_n is connected, we get that $f_n\left(\frac{x-u}{\nu}\right) > 0$ for all $u \in [\sigma, \tau]$.

So finally assume that $0 < p_0(u) = p_0\left(u + \frac{s}{2}\right) < 1$ and define $\tau = u + \frac{s}{2}$ as well as $\sigma = \tau - \frac{d}{2}$. Because of our gap inequality, assumed to hold for p_0, it is clear that $p_0(\sigma) < p_0(\tau)$ must hold. $f_n\left(\frac{x-\tau}{\nu}\right) > 0$ as before. Note that $\frac{I_n^- + I_n^+}{2} = I_n^- + \frac{d}{2\nu}$ and that $I_n^- + \frac{d}{\nu} = I_n^+$. Above we already saw that $I_n^- < \frac{x-\tau}{\nu} < I_n^- + \frac{d}{2\nu}$. Thus $I_n^- + \frac{d}{2\nu} < \frac{x-\sigma}{\nu} < I_n^+$, and because f_n is positive on (I_n^-, I_n^+), we get that $f_n\left(\frac{x-\sigma}{\nu}\right) > 0$. Thus in this case, the σ and τ as chosen also satisfy the requirements. □

Let's consider the effect of noise by example. Figure 4 is the analogue of Figure 2 with Figure 2b as original and increasing amount of noise (with a Gaussian distribution) added to it. In the sequence Figure 4d, Figure 4e and Figure 4f, it is clearly visible that the noise removes the discontinuities present in Figure 2e, makes p_ν ever smoother and also washes out the constant regions, thus demonstrating Theorem 19 in practice. Note that the minima of the cost functions are kept in place, and so a segmentation found on the noisy, smooth functions is also applicable to the original image in this case; see also Figure 8 later.

(a) 2 % noise.

(b) 5 % noise.

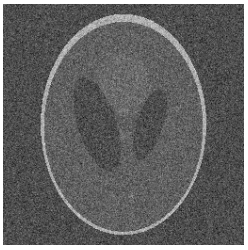

(c) 20 % noise.

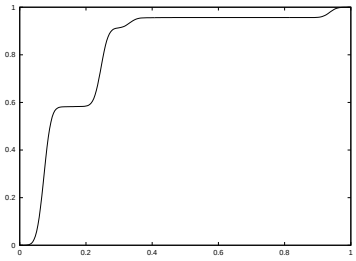

(d) Distribution p_ν.

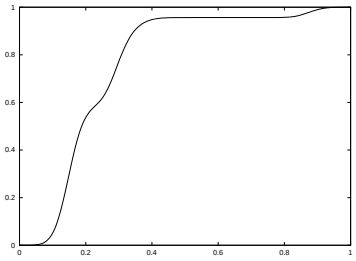

(e) Distribution p_ν.

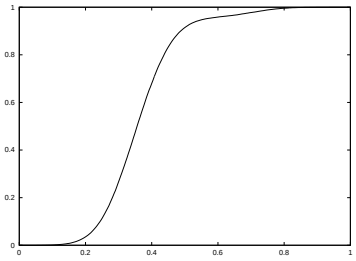

(f) Distribution p_ν.

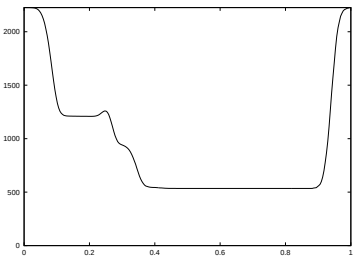

(g) Cost K_{p_ν} for $M = 2$.

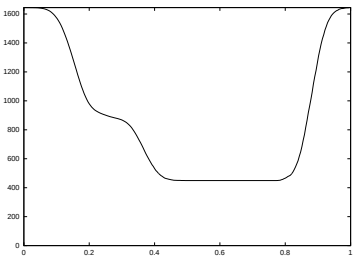

(h) Cost K_{p_ν} for $M = 2$.

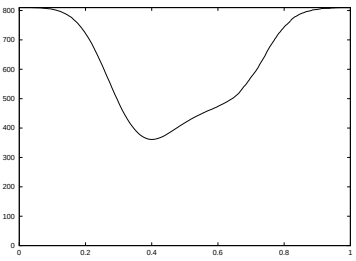

(i) Cost K_{p_ν} for $M = 2$.

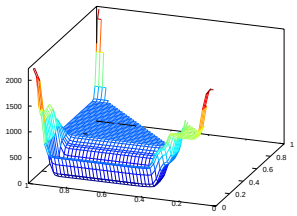

(j) Cost K_{p_ν} for $M = 3$.

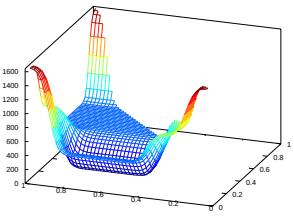

(k) Cost K_{p_ν} for $M = 3$.

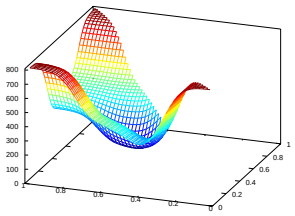

(l) Cost K_{p_ν} for $M = 3$.

Figure 4: Effect of noise added to image.

6 Remarks about Implementation

In practice, while an image can be considered as a map like $u : [0,1] \times [0,1] \to [0,1]$, it is given as a discretized version. The domain is usually decomposed into a finite number of pixels (that are then organized in a two-dimensional grid); let for the rest of this section the number of pixels of some image considered be $N = N'^2$ (where N' is the image's width and height).

In addition, the intensity u_i corresponding to some pixel $i = 1, \dots, N$ has to be stored on a computer in some way. This can be done either as a floating-point number, say, $u_i \in [0,1]$ (with very fine division into distinct, possible values), but often this is even done as integer number in a given range $u_i = 0, \dots, I-1$ which can be seen as an approximation to $\tilde{u}_i = \frac{u_i}{I-1} \in [0,1]$. Common choices are $I = 256 = 2^8$ or $I = 2^{16}$ (8 bit or 16 bit gray-scale images, respectively). Note that I is used in this section as number of intensities, while the set of possible intensities will be denoted as $\mathcal{I}$.

Below, I will consider both situations (floating-point (nearly) continuous intensities and "few" discrete pixel values) and describe how to possibly apply the analysis done and methods described above for them efficiently. As above, I will concentrate on finding a good segmentation as a set of boundaries $b \in B$ in intensity-space. From there on it is straight-forward to construct the segmented image, of course.

6.1 Preparations

All I need for my analysis is not the real image u, including for instance topological properties of the domain or information about neighbourship of certain pixels, but instead only the function p, essentially giving details about "how much" of each intensity is there in the image. Thus we can also in the practical case transform the image from a grid of pixels into more efficient forms.

In case of floating-point intensities, the preparation I suggest is to use Algorithm 1: Put all intensities into a one-dimensional array and sort it. This can be done with time-complexity $\mathrm{O}(N \log N)$ by some of the usual efficient sorting algorithms, for instance merge-sort or heap-sort. The memory usage is then exactly the same as storing the original image, so no additional impact. I will in the following assume that $u_i \le u_j$ for $1 \le i < j \le N$, which represents the image processed in this way.

Algorithm 1 Preparation for floating-point intensities.

Require: Ω is a finite domain with $|\Omega| = N$, $\tilde{u}_x \in \mathcal{I}$ for $x \in \Omega$ are the intensities
Ensure: $u = (u_1, \dots, u_N)$ is a permutation of $\tilde{u}$ such that $u_1 \le u_2 \le \dots \le u_N$
1: $u \leftarrow$ empty list
2: **for all** $x \in \Omega$ **do**
3: add $\tilde{u}_x$ to the list u
4: **end for**
5: sort the list u

If the number of possible intensities I is rather small (say $I \ll N$) — as in the integer-range case, especially with 8 bit pixels —, it seems beneficial to build up a histogram instead. That is, for each possible intensity value, count how many pixels there are of some intensity:

$$n_t = |\{i = 1, \dots, N \mid u_i = t\}| \tag{18}$$

for $t \in \mathcal{I}$; but because this set is finite, we'll assume $t = 0, \dots, I-1$ in the following. This is described in Algorithm 2. It has time-complexity $\mathrm{O}(N)$ (as one must walk through the image once) and uses memory of the order $\mathrm{O}(I)$, thus even less than the full image.

6.2 dp Integrals

Obviously, it is very important to calculate integrals such as

$$J(\sigma, \tau, f) = \int_\sigma^\tau f \, dp = \int_{(\sigma,\tau]} f \, dp \tag{19}$$

for our discrete images. Note that because of the discretization, it is now important to specify the range exactly — $(\sigma, \tau]$ instead of $[\sigma, \tau]$ as convention from now on. Those are no longer the same, as p can no longer be *exactly* smooth or continuous!

For numerical calculation, we'll consider Equation 19 in the Riemann-Stieltjes sense. Then let i, j be given such that

Algorithm 2 Preparation for integer intensities.

Require: $|\Omega| = N$ and $|\mathcal{I}| = I$ are finite, $u_x \in \mathcal{I}$ for $x \in \Omega$ are the intensities
Ensure: for all $t \in \mathcal{I}$, n_t satisfies Equation 18
1: **for all** $t \in \mathcal{I}$ **do**
2: $\quad n_t \leftarrow 0$
3: **end for**
4: **for all** $x \in \Omega$ **do**
5: $\quad$ increment n_{u_x}
6: **end for**

- $\sigma < u_i \leq u_j \leq \tau$,
- $u_k \leq \sigma$ for all $k < i$ and
- $u_l > \tau$ for all $l > j$.

Such i and j can be found using binary search on the sorted array of intensities with time-complexity $\mathrm{O}(\log N)$. If this is done, it should be clear that the integral will be defined as

$$J(\sigma, \tau, f) = \frac{1}{N} \sum_{k=i}^{j} f(u_k). \tag{20}$$

Thus, for floating-point intensities, the cost of one *dp* integration is roughly $\mathrm{O}(\log N + N) = \mathrm{O}(N)$ (assuming that the number of pixels with intensity in the range of integration is of the same order of magnitude as the overall number of pixels (N), which seems reasonable for the complexity estimation).

If there are only few intensities and a histogram is available, Equation 20 reduces to

$$J(\sigma, \tau, f) = \frac{1}{N} \sum_{t=\sigma+1}^{\tau} n_t f(t). \tag{21}$$

This is even cheaper to calculate, namely of the order $\mathrm{O}(I)$.

Note that clearly for $\sigma < \tau < \rho$, we have

$$J(\tau, \rho, f) = J(\sigma, \rho, f) - J(\sigma, \tau, f). \tag{22}$$

Thus, if the function f is fixed but we need to calculate a lot of those integrals for different boundaries, we can speed calculation up via precalculation. Let $\sigma < I^- = u_1$ be some lower bound for all intensities, then calculate the values of $J(\sigma, x, f)$ for all distinct intensities x that appear in the image — those are at most N or I, depending on the type of image present. Because the sums in Equation 20 or Equation 21 can be built up cumulatively for this (see Algorithm 3 and Algorithm 4), the total time-complexity of this precalculation is also only $\mathrm{O}(N)$ or $\mathrm{O}(I)$, respectively.

Algorithm 3 Precalculation of integral for floating-point intensities.

Require: u_i for $i = 1, \ldots, N$ as per Algorithm 1, a mapping $f : \mathcal{I} \to \mathbb{R}$
Ensure: $a_i = J(\sigma, u_i, f)$ for $i = 1, \ldots, N$ and all $\sigma < u_1$
1: $a_0 \leftarrow 0$
2: **for** $i = 1, \ldots, N$ **do** ▷ Calculate Equation 20 successively.
3: $\quad a_i \leftarrow a_{i-1} + \frac{f(u_i)}{N}$
4: **end for**

When this is done, $J(\tau, \rho, f) = J(\sigma, \rho, f) - J(\sigma, \tau, f)$ can be calculated via two cheap look-ups. For the floating-point intensity case, we still need to do the binary search, thus the cost of one integration after doing the precalculation is then $\mathrm{O}(\log N)$; for a histogram image, it is even $\mathrm{O}(1)$! This procedure can be compared to finding the indefinite integral (anti-derivative) of a function in order to later derive the definite integral (maybe for a set of different boundaries) from it.

As a final remark: It may be necessary to calculate an integral as in Equation 19 more precisely with respect to the boundaries; that is, in a way such that $J(\sigma, \tau, f) < J(\sigma, \tau', f)$ for $\tau < \tau'$ even if there is no pixel u_i in the image in-between (such that for instance $\tau \leq u_i < \tau'$). This property corresponds to the condition $p'(t) > 0$ we had to introduce in Section 4 to ensure nice behaviour; if this is not done, then the methods described above may (and do in practice) not work well, as the theoretic assumptions are violated.

Algorithm 4 Precalculation of integral with available histogram.

Require: n_t as per Algorithm 2, a mapping $f : \mathcal{I} \to \mathbb{R}$
Ensure: $a_t = J(\sigma, t, f)$ for $t \in \mathcal{I}$ and all $\sigma < \inf \mathcal{I}$

$s \leftarrow 0$
for $t \in \mathcal{I}$ in increasing order **do** ▷ Calculate Equation 21 successively.
  $s \leftarrow s + \frac{n_t f(t)}{N}$
  $a_t \leftarrow s$
end for

In this case, if i is the largest value such that we have $u_i < \tau < u_{i+1}$, we can do a linear interpolation between $J(\sigma, u_i, f)$ and $J(\sigma, u_{i+1}, f)$ and set for $\lambda = \frac{\tau - u_i}{u_{i+1} - u_i} \in (0, 1)$ the integral as

$$J(\sigma, \tau, f) = (1 - \lambda) J(\sigma, u_i, f) + \lambda J(\sigma, u_{i+1}, f) = J(\sigma, u_i, f) + \lambda \frac{f(u_{i+1})}{N}. \tag{23}$$

This can be calculated as efficiently as the original case. By using Equation 22, the lower boundary can just as well be some arbitrary value. Finding a particular integral with interpolation based on a precalculation is formalized in Algorithm 5. Of course this is not necessarily a very precise interpolation, but it does ensure strict monotonicity, which gets lost if we use only the individual pixels or even just the histogram with few different values (which effectively behaves as if p were a step-function).

Algorithm 5 Finding a dp integral based on precalculation.

Require: a mapping $f : \mathcal{I} \to \mathbb{R}$ and precalculation done for f according to Algorithm 3 or Algorithm 4
Ensure: for $I^- \leq \sigma < \tau \leq I^+$, INTEGRATE$(\sigma, \tau, f)$ returns $J(\sigma, \tau, f)$ as described in the text

procedure INT_UPPER(τ, f) ▷ Find integral on $[I^-, \tau]$.
  if floating-point intensities **then**
    find largest i such that $u_i \leq \tau$ with binary search
    $t \leftarrow a_i$ ▷ This is the precalculated value.
    if $u_i < \tau$ **then**
      $\lambda \leftarrow \frac{\tau - u_i}{u_{i+1} - u_i}$
      $t \leftarrow t + \lambda \frac{f(u_{i+1})}{N}$ ▷ As per Equation 23.
    end if
    return t
  else
    find largest $s \in \mathcal{I}$ such that $s \leq \tau$ ▷ For instance, by rounding τ to an integer.
    if $s = \tau$ **then**
      return a_s ▷ This is the precalculated value.
    else
      find smallest $t \in \mathcal{I}$ with $s < \tau < t$ ▷ May be $t = s + 1$.
      $\lambda \leftarrow \frac{\tau - s}{t - s}$
      return $(1 - \lambda) a_s + \lambda a_t$
    end if
  end if
end procedure
procedure INTEGRATE(σ, τ, f)
  return INT_UPPER(τ, f) − INT_UPPER(σ, f) ▷ Application of Equation 22.
end procedure

The integrals that are really needed to carry out segmentation either by fixed-point iteration or the sequential construction of Theorem 17 are those for the functions $f(t) = t$ and $f(t) = 1$. With those two, $c_p((\sigma, \tau])$ can be calculated as in Definition 5. Thus, we should precalculate the integrals for those two functions. This again has a time-complexity of $\mathrm{O}(N)$ or $\mathrm{O}(I)$ and is thus also not any more expensive than just walking over the image once.

6.3 Fixed-Point Iteration

If a set of boundaries $b^{(n)} \in B$ is given, with the methods described in Subsection 6.2 we can easily implement the fixed-point iterations described in Subsection 4.3. All that is needed to calculate $b^{(n+1)}$ from $b^{(n)}$ is calculation of different values of $c_p\left(\left(b_i{}^{(n)}, b_{i+1}{}^{(n)}\right]\right)$.

As was already mentioned there, I see two possible implementations based on Definition 7: Either with Φ that calculates all components of the new segmentation boundaries "at once" (similar to the Jacobi iteration method for solving linear systems), or based on the functions Ψ_i and updating one component at a time (in the spirit of the Gauß-Seidel method). In the latter case, there's also the choice of order in which the updates are done — say, forward, backward or symmetric (one forward sweep followed by a backward one).

In order to apply such an iteration scheme, there are still two points worth mentioning: Getting an initial guess and a reasonable stopping criterion. As initial segmentation, I suggest to use one sequentially constructed as described below in Subsection 6.4. Alternatively, a simpler method which also worked quite well in tests is to use equi-sized initial segments, either in intensity-space (such that ${b_{i+1}}^{(0)} - {b_i}^{(0)} = \frac{I^+ - I^-}{M}$ holds for $i = 0, \ldots, M-1$) or in the original image domain (using the quantile values of p, that is, such that $p({b_i}^{(0)}) = \frac{i}{M}$).

For the stopping criterion, for a given tolerance $\epsilon > 0$, one can do the iteration until

$$\left\| b^{(n+1)} - b^{(n)} \right\| < \epsilon \tag{24}$$

holds for some suitable norm or a maximum number of iterations has been reached. It must be noted at this point that without the linear interpolation seen in Equation 23, it may (and eventually probably will) happen that $b^{(n+1)} = b^{(n)}$ holds exactly even when not yet at a fixed-point because the integrals underlying the iteration update result in exactly the same values despite small changes in the boundaries. In that case, this can be used as a stopping-criterion as well — but I suggest to do the linear interpolation and use Equation 24. The fixed-point iteration with Gauß-Seidel update and linear interpolation is detailed in Algorithm 6.

Algorithm 6 Segmentation via Gauß-Seidel type fixed-point iteration.

Require: integral precalculation for $f(t) = 1$ and $f(t) = t$ done via Algorithm 3 or Algorithm 4, let $\epsilon > 0$, $M \geq 2$ and assume that $b_1 < \cdots < b_{M-1}$ is an initial segmentation
Ensure: $b = (b_1, \ldots, b_{M-1})$ is an approximate fixed-point of Φ fulfilling Equation 24 with $\|\cdot\|_\infty$

```
procedure CP(σ, τ)                                  ▷ Calculate c_p((σ, τ]) according to Definition 5.
    d ← INTEGRATE(σ, τ, t ↦ 1)                      ▷ Procedure defined in Algorithm 5.
    if d = 0 then
        return σ
    else
        return (1/d) · INTEGRATE(σ, τ, t ↦ t)
    end if
end procedure
repeat
    δ ← 0
    for i = 1, ..., M − 1 do                        ▷ Perform b → Ψ_i(b) as per Definition 7.
        c_p^{i−1/2} ← CP(b_{i−1}, b_i)
        c_p^{i+1/2} ← CP(b_i, b_{i+1})
        b' ← (c_p^{i+1/2} + c_p^{i−1/2}) / 2
        δ ← max(δ, |b_i − b'|)
        b_i ← b'
    end for
until δ < ε
```

For each component-update in the fixed-point iteration, $c_p^{i+\frac{1}{2}}$ and $c_p^{i-\frac{1}{2}}$ have to be calculated. If doing the update with Φ, most of them can be used to calculate the updates of both the lower and upper neighbouring boundary to speed up the calculation by (nearly) a factor of two. Overall, however, for each component a fixed number of integrals has to be calculated. Taking precalculation for those into account, the time cost of each fixed-point iteration is for the floating-point intensity case $\mathrm{O}(M \log N)$ and for histogram images $\mathrm{O}(M)$. Both of them are rather cheap.

6.4 Sequential Construction of a Fixed-Point

The same sequential construction that is used in the proof of Lemma 16 can be applied numerically quite efficiently to find a solution to Equation 13 directly. Because of rounding errors and even more so

the discrete nature of the image that makes solution of Equation 15 inexact, the result is however not as good as one might hope. Especially as the construction works "forward" from one component to the next, the last components will be even more inexact than the first ones, as calculational error cumulates from b_2 onwards up to b_{M-1}. Thus, I suggest to use this procedure to obtain a starting-point for a fixed-point iteration whose result is actually delivered later as the segmentation.

First, I'll consider the construction of subsequent boundaries if the first one is given. As this is done successively, it is without loss of generality enough to assume $b_0 \leq b_1$ given and show how to construct $b_2 = \beta_2(b_1)$ (with the notation of Lemma 16). When b_0 and b_1 are given, $c_p^{1-\frac{1}{2}} = c_p((b_0, b_1])$ can be calculated by means of integration as usual. Then we know what $c_p^{1+\frac{1}{2}} = c_p((b_1, b_2])$ must be, namely $c_p^{1+\frac{1}{2}} = b_1 + (b_1 - c_p^{1-\frac{1}{2}})$. Because $c_p((b_1, b_2])$ is strictly increasing with respect to b_2 for fixed b_1, the solution b_2 can be found with interval bisection. Each step during the bisection costs as much as dp integration costs, thus $\mathrm{O}(\log N)$ or $\mathrm{O}(1)$. The number of necessary steps clearly depends on the precision sought, but will probably be around the order $\mathrm{O}(\log N)$ or $\mathrm{O}(\log I)$. Thus construction of b_2 costs $\mathrm{O}\left(\log^2 N\right)$ for floating-point intensities and $\mathrm{O}(\log I)$ for histogram images.

All together we have to construct not only b_2 but all following b_i's as well, this takes $M-1$ times as long — leading to $\mathrm{O}\left(M \log^2 N\right)$ or $\mathrm{O}(M \log I)$, respectively, for constructing all boundaries from a given first one. This construction of $b_2, \ldots, b_{M-1}$ from b_1 is given by Algorithm 7.

Algorithm 7 Construction of subsequent boundaries of a fixed-point.

Require: precalculation of integrals done as also required by Algorithm 6, $b_0 = I^-$, $b_1 \in \mathcal{I}$ is given

Ensure: if b_1 is small enough, $b_2, \ldots, b_{M-1}$ satisfy $b_i = \frac{c_p^{i+\frac{1}{2}} + c_p^{i-\frac{1}{2}}}{2}$ for all $i = 1, \ldots, M-2$

```
for i = 2, ..., M − 1 do
    c ← 2b_{i−1} − CP(b_{i−1}, b_{i−2})          ▷ Procedure defined in Algorithm 6.
    if CP(b_{i−1}, I^+) < c then
        return failure                            ▷ Can happen if b_1 is too large.
    else
        find root t of function s ↦ CP(b_{i−1}, s) − c with interval bisection
        b_i ← t
    end if
end for
```

Finally we want to find a fixed-point without already knowing what b_1 is. We have to find a suitable b_1 such that after doing the construction just described also $b_{M-1} = \frac{c_p^{M-1+\frac{1}{2}} + c_p^{M-1-\frac{1}{2}}}{2}$ holds. (Put another way, the b_M given by the construction should actually match the upper boundary I^+ of intensities.) For this, as in the proof of Theorem 17, note that for very small b_1, the last boundary will be less than what it should be; and for large b_1, it will be too large. Thus again, a binary search for b_1 will reveal a matching one. As before, roughly $\mathrm{O}(\log N)$ or $\mathrm{O}(\log I)$ steps are necessary in this search. So, we can sequentially construct a fixed-point with time-complexity $\mathrm{O}\left(M \log^3 N\right)$ or $\mathrm{O}\left(M \log^2 I\right)$ according to Algorithm 8.

When there are more than just one fixed-points, the sequentially constructed $b \in B$ may not be the solution to our segmentation problem. But note that for the task of segmentation, it is just important to find out which pixels should belong to which segment. Thus the boundaries have to be specified only up to a precision such that they separate individual pixels or histogram-entries. Thus, an alternative approach is to try all N or I intensities present in the image as b_1 and pick those that satisfy the fixed-point criterion. Among the resulting fixed-points, the optimal segmentation is that which results in the lowest cost-value. For this extended algorithm, the complexity becomes $\mathrm{O}\left(MN \log^2 N\right)$ for floating-point intensities and $\mathrm{O}(MI \log I)$ for histograms. This is of course more expensive than the binary-search approach, but still (especially for a low number M of segments) basically of the same order of magnitude than going over all pixels once, which clearly is the "absolute minimum" for any image processing.

6.5 Finding Fixed-Points Summarized

So summarizing what was described in the previous subsections: First of all, for a given image as set of pixels, in a preparation sweep those pixels have to be sorted or counted into histogram bins, see Algorithm 1 and Algorithm 2. Then, with Subsection 6.4 and Algorithm 8 a fixed-point (or multiple fixed-points) can be sequentially constructed; alternatively, one can obtain some other initial segmentation. When this is done, I suggest starting there with the fixed-point iteration described in Subsection 4.3 and

Algorithm 8 Sequential construction of a fixed-point of Φ.

Require: precalculation of integrals done as also required by Algorithm 6
Ensure: $b = (b_1, \ldots, b_{M-1})$ is a fixed-point

procedure ERROR(b_1) ▷ Positive if b_1 is too large and negative if b_1 is too small.
  construct $b_2, \ldots, b_{M-1}$ as per Algorithm 7
  if construction failed **then**
    return ∞ ▷ This means that b_1 is too large.
  else
    $c_p^{M-1-\frac{1}{2}} \leftarrow \mathrm{CP}(b_{M-2}, b_{M-1})$ ▷ Procedure defined in Algorithm 6.
    $c_p^{M-1+\frac{1}{2}} \leftarrow \mathrm{CP}(b_{M-1}, I^+)$
    return $b_{M-1} - \frac{c_p^{M-1+\frac{1}{2}} + c_p^{M-1-\frac{1}{2}}}{2}$
  end if
end procedure
find root b_1 of function $\theta \mapsto \mathrm{ERROR}(\theta)$ with interval bisection
construct $b_2, \ldots, b_{M-1}$ as per Algorithm 7 ▷ This will never fail for a root.

Algorithm 6 to refine the initial boundaries further. Finally, from the boundaries in intensity-space it is trivial to calculate the corresponding segments' sub-domains and intensities, to get a segmented image. This is put together in Algorithm 9.

Algorithm 9 Full algorithm for image segmentation as described herein.

Require: $u : \Omega \to \mathcal{I}$ is an image where Ω and $\mathcal{I}$ are finite sets, $M \geq 2$ is given
Ensure: s is a segmentation of u with M segments

do preparation with Algorithm 1 or Algorithm 2
precalculate integrals with Algorithm 3 or Algorithm 4 for the functions $f(t) = 1$ and $f(t) = t$
$b_0 \leftarrow I^-$, $b_M \leftarrow I^+$
construct $b = (b_1, \ldots, b_{M-1})$ with Algorithm 8
call Algorithm 6 on b
$s \leftarrow$ empty image
for $i = 1, \ldots, M$ **do**
  $c \leftarrow \mathrm{CP}(b_{i-1}, b_i)$ ▷ Optimal segment-intensity per Theorem 2.
  for all $x \in \Omega$ with $b_{i-1} < u_x \leq b_i$ **do** ▷ Twice non-strict inequality if $i = 1$.
    $s_x \leftarrow c$
  end for
end for

As I think this is the most common case, let's consider an image with I different intensities (rather than unconstrained floating-point values for intensities with a lot of different possibilities). Then the preparation building up the histogram with $\mathrm{O}(N)$ is the most expensive step. Every later one does not depend at all on the image size N, but only the number I of histogram bins. With $I = 256$ as a usual value, this is very cheap. Reduction of the original image to only its distribution function p (or in this case, the histogram) gives a very significant performance improvement compared to working with the original grid of pixels.

6.6 Adding Noise

By Theorem 19 we saw that adding noise to an image helped to ensure that the resulting distribution function is natural. While for a lot of "real" images this criterion will usually already be fulfilled (either because the image is smooth in itself or because there is already some amount of noise captured with the image "automatically"), sometimes it may even be helpful to add noise artificially in order to mollify p. For images like Figure 2b, the methods detailed in this section do not work properly because over a wide range changing the segment boundaries has no effect at all on the segmentation or c_p values as there are only a very small number of intensities actually used in the image — and thus p is discontinuous and flat.

If this is the case, as can be seen in Figure 4 it helps a lot to add noise and segment the resulting image instead. A possible strategy is to add a rather large level of noise, find the corresponding segmentation; then add a smaller amount of noise to the original image and refine the found segmentation with a number of fixed-point iterations, and so on — successively reducing the amount of noise added, until

the image processed already comes very close to the original. This process works well for Figure 2b as can be seen in Section 7 and will probably do so for a lot of similar cases. However, one must be aware that theoretically there is no guarantee that a small change in the noise level only changes the optimal solution slightly. In fact, while the cost function depends continuously on the noise level added, its global minimum might not. For practical purposes though, it is at least worth a try in case the segmentation methods are found to be inefficient or divergent for the original image.

I also want to remark that in order to add noise to the image, it is not necessary to do so on the original set of pixels. Instead, suppose the image is first transformed into a histogram of intensities — note that the histogram corresponds to the density p' instead of the distribution p. Then a smoothed histogram, corresponding to an image with noise added, can be calculated directly via a numerical convolution of the original histogram with the density function of the noise. This convolution can be compared to Equation 17 and motivated in a way similar to the proof of Lemma 18, where the distribution p is smoothed.

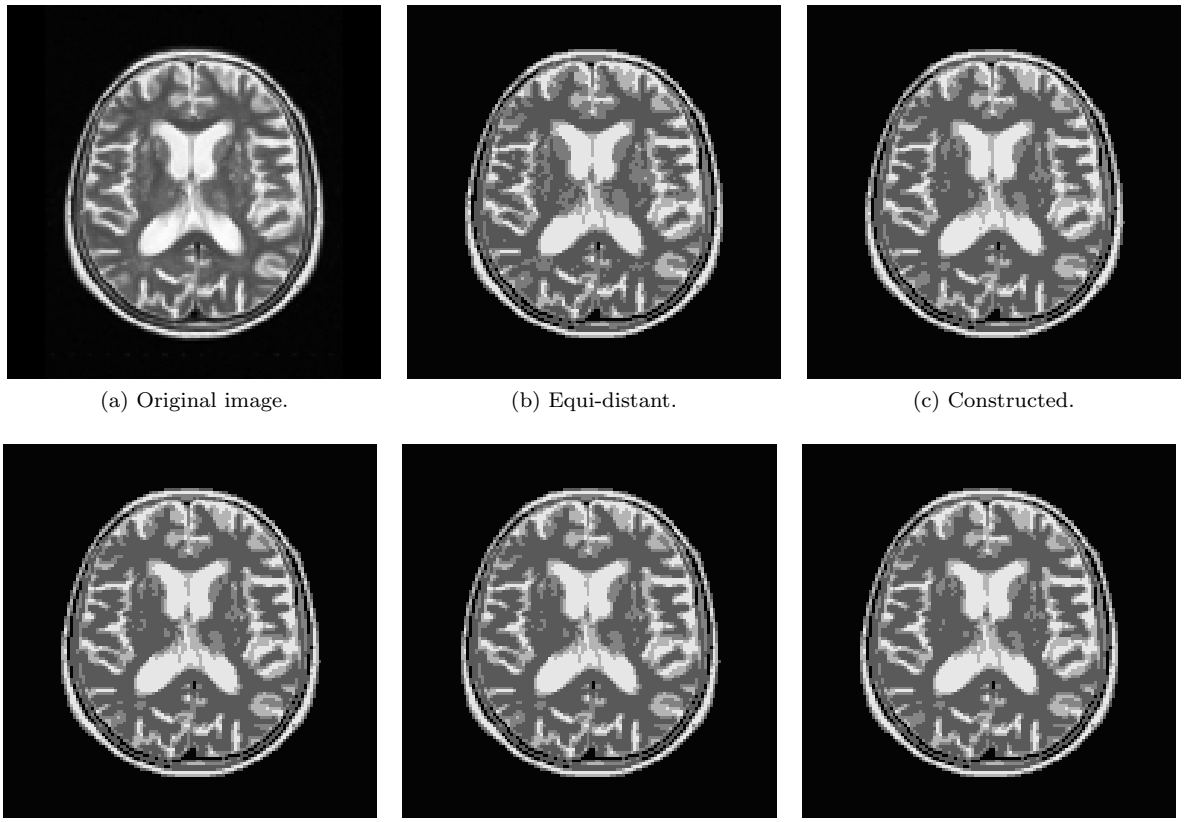

(a) Original image. (b) Equi-distant. (c) Constructed.

(d) Iteration equi-distant. (e) Iteration constructed. (f) Method of [7].

Figure 5: Segmentation results for MR image.

7 Computational Results

For the histogram case (in particular, using 8 bit gray-scale) I implemented the methods described in Section 6 with GNU Octave [1]. In this section I will present the results. Computation was done on a GNU/Linux system with Octave 3.0.3, Mobile AMD Sempron 3100+ processor and 512 MiB of RAM. As discussed in Section 6, time-complexity is not the limiting factor for my algorithms, thus the code was not implemented in the most efficient manner. Additionally, Octave is an interpreted platform also not very efficient for certain patterns. What is more important are the quantitative results with respect to number of fixed-point iterations and minimum cost at the solution.

I always used 128×128 pixel images with integer intensities in the range 1–256. Segmentation was done targeting $M = 5$ different segments. For the fixed-point iteration, I used $\left\|b^{(n+1)} - b^{(n)}\right\|_\infty < 10^{-3}$ as stopping criterion (boundaries are equally effective when rounded to integers, thus this stopping criterion gives much more precision than actually necessary); for the sequential fixed-point construction, the tolerance for interval bisections was chosen as 10^{-6}.

First, I constructed two initial segmentations: One with equi-distant boundaries (called "Equi-distant" in the result tables and figures) and one with the sequential fixed-point construction as in Subsection 6.4, called "Constructed". Then I used fixed-point iteration with the "Jacobi" and with the "Gauß-Seidel" style, starting from those two initial values. These results are listed as "Iteration equi-distant" and "Iteration constructed", respectively. As a comparison, I also used the segmentation method described in [7, p. 9] with $\gamma = 0.5$ and $\mu_t = 10^{-3}$.

Note that the "Jacobi" and "Gauß-Seidel" iterations always resulted in precisely the same result, and only the number of iterations is different (fewer needed for the latter type). Because of this, I will always combine those two in the results below.

The image in Figure 5a is seemingly very easy to segment, all result images in Figure 5 look rather nice (even that where just the equi-distant boundaries are used without further processing). In Table 1, it can be seen that also the resulting segmentation qualities are nearly the same, although the fixed-point methods (from both starting points alike) slightly beat the sequential fixed-point construction alone and the method of [7]. The solution boundaries are also nearly identical for both fixed-point methods (they

	Result Cost	Iterations Jacobi / GS	Solution Boundaries
Equi-distant	100.17		51.20, 102.40, 153.60, 204.80
Constructed	96.87		47.31, 111.00, 158.49, 211.43
Iteration equi-distant.	95.95	43 / 36	47.31, 110.33, 155.89, 206.08
Iteration constructed.	95.95	45 / 39	47.31, 110.33, 155.91, 206.10
Method of [7].	97.13		

Table 1: Segmentation results for MR image.

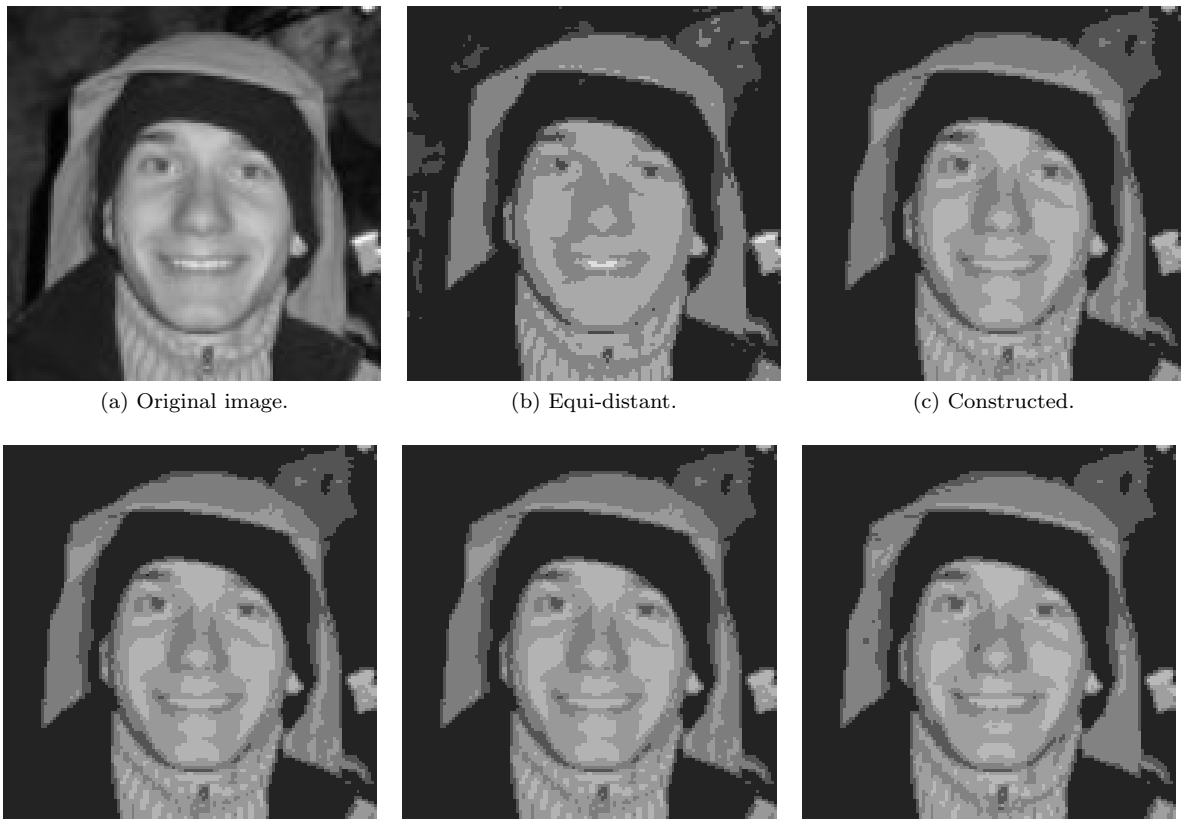

(a) Original image. (b) Equi-distant. (c) Constructed.

(d) Iteration equi-distant. (e) Iteration constructed. (f) Method of [7].

Figure 6: Segmentation results for a natural picture.

are the same when rounded), but with the boundaries of the sequentially constructed fixed-point without refinement it can be seen that the boundaries get more and more inexact the larger their indices are (this is the result of error accumulation while successively constructing the boundaries from smaller to larger ones).

The natural image in Figure 6 shows more variation and gradients than Figure 5a, and it can be seen that in this case the trivial segmentation with equi-distant segments alone is not as good as the other methods; for instance, it does not capture the face as well and also introduces more artefacts in the background. The cost-landscape of this image is defined very clearly, and so all methods including the sequential fixed-point construction result at nearly the same segmentation (as can be verified from Table 2). The method of [7] is slightly (but notably) worse with respect to the cost; there are also some visible differences between Figure 6f and Figure 6e, although it is probably not clear to define any one of those as "visually better" than the other.

For the phantom image Figure 7a, the results in Figure 7 are pretty bad visually. The problem here is that the image's distribution function p (as seen in Figure 2e) is rather irregular (completely flat except for a few discontinuities). As can be seen in Table 3, the iterations applied starting from the equi-distant initial condition change the boundaries, but the cost is unaltered. This is because all change takes place within the flat regions only, where it does not affect anything at all. The sequential fixed-point construction failed completely to identify a good result for similar reasons. Note however

	Result Cost	Iterations Jacobi / GS	Solution Boundaries
Equi-distant	147.91		51.20, 102.40, 153.60, 204.80
Constructed	112.67		60.43, 105.66, 139.73, 166.60
Iteration equi-distant.	112.67	52 / 45	60.43, 105.67, 139.74, 166.60
Iteration constructed.	112.67	1 / 1	60.43, 105.66, 139.73, 166.60
Method of [7].	117.36		

Table 2: Segmentation results for a natural picture.

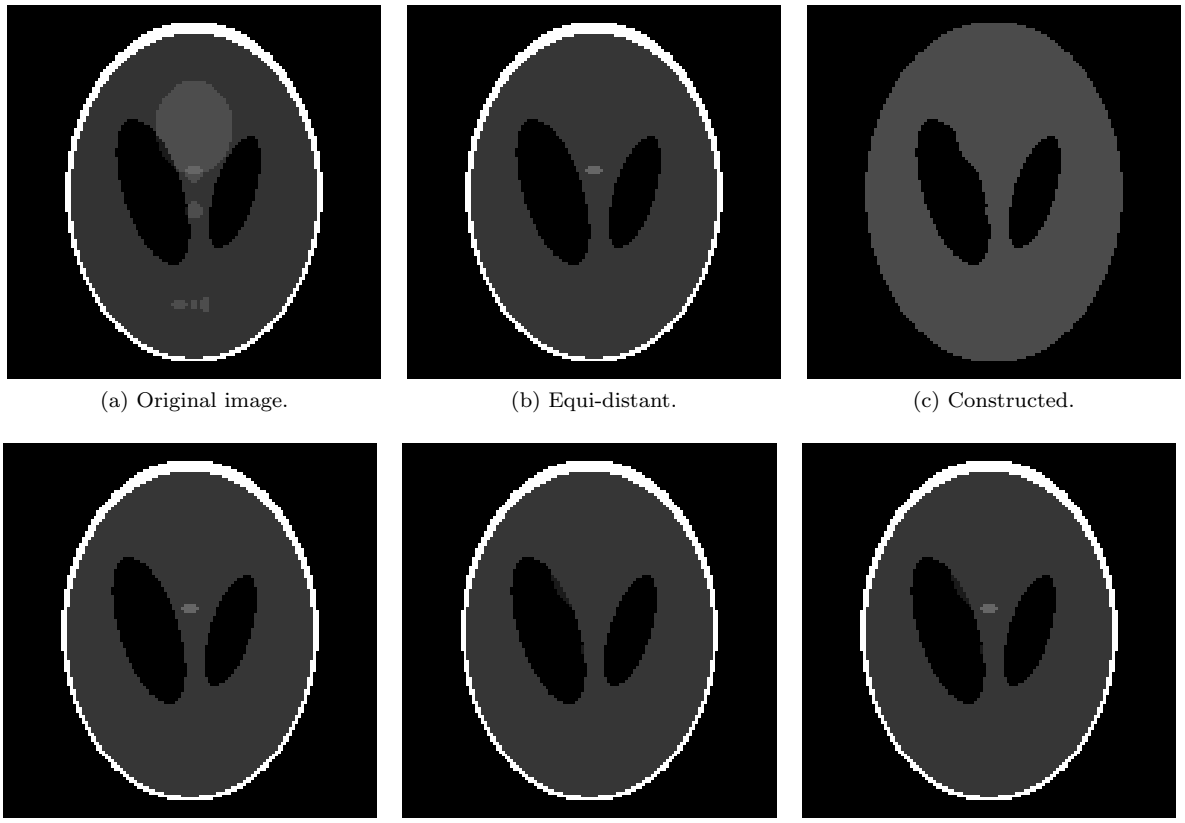

(a) Original image. (b) Equi-distant. (c) Constructed.

(d) Iteration equi-distant. (e) Iteration constructed. (f) Method of [7].

Figure 7: Segmentation results for original phantom image.

	Result Cost	Iterations Jacobi / GS	Solution Boundaries
Equi-distant	26.56		51.20, 102.40, 153.60, 204.80
Constructed	1584.61		13.96, 26.00, 26.00, 26.00
Iteration equi-distant.	26.56	16 / 16	28.04, 79.01, 103.00, 179.50
Iteration constructed.	27.54	5 / 5	14.00, 27.00, 41.06, 155.56
Method of [7].	25.57		

Table 3: Segmentation results for phantom image.

(a) Noisy image. (b) Equi-distant. (c) Constructed.

(d) Iteration equi-distant. (e) Iteration constructed. (f) Method of [7].

Figure 8: Segmentation results for phantom image with 1 % of noise added.

	Result Cost	Iterations Jacobi / GS	Solution Boundaries
Equi-distant	25.56		51.20, 102.40, 153.60, 204.80
Constructed	1.51		32.97, 58.23, 75.00, 244.53
Iteration equi-distant.	0.99	5 / 5	33.62, 69.49, 93.38, 177.12
Iteration constructed.	1.51	3 / 3	32.97, 58.23, 71.11, 165.45
Method of [7].	6.53		

Table 4: Segmentation results for phantom image with 1 % of noise added.

that also the method of [7] did not reproduce the original image as well as it possibly could have done. As the image consists only of 5 different intensities, the segmentation can be optimal in theory.

If we add only 1 % of noise to the phantom image, results are much better (as predicted in the analysis in Section 5). Figure 8a is the noisy version of Figure 7a, and for Figure 8b to Figure 8e, the segmentation boundaries were calculated with the respective methods based on the noisy image, but then applied to the original one. The method of [7] was applied to the noisy image to get Figure 8f, and here the noise also helped to improve greatly on Figure 7f. The costs in Table 4 are calculated as $\|u - s\|^2_{\mathrm{L}^2}$ based on the reconstructed images rather than via $K_p(b)$ and the boundaries, in order to give meaningful results for this case. Both the sequential fixed-point construction in Figure 8c and the iteration methods in Figure 8d give very good results, as does the method of [7]. The result of the fixed-point iteration starting from the equi-distant segmentation is "perfect" visually and has slightly lower cost than the sequentially constructed fixed-point, which results in the same segmentation as the fixed-point iteration starting from it. These two possibilities are seemingly distinct fixed-points (local minima) leading to slightly different results.

8 Conclusion

In the preceding sections, I have formulated the problem of image segmentation using probabilistic techniques in intensity-space. As consequence, instead of optimizing the shape of segment sub-domains (which is an infinite-dimensional problem) I only have to consider boundaries between segments given as intensities. As I only consider gray-scale images, this is very easy and leads to a finite-dimensional optimization problem. For this problem, the optimality system can be derived and takes a very nice form. In particular, solving the system with a fixed-point iteration corresponds to the well-known k-means clustering algorithm applied to image segmentation. This means, that my work gives a measure theoretic derivation and justification of this algorithm in certain segmentation cases.

While not all images are suitably smooth and regular for my purposes, I showed that if random noise is applied to any image (either artificially exactly for that purpose or by the practical measurement that was used to obtain the image to process), the necessary conditions are satisfied. So for practical purposes, the methods described can be applied.

The segmentation algorithms proposed are very efficient, because the reformulation also gives algorithmic advantages. Especially for the common case of images represented with a small number of possible gray-levels (like 256 for 8 bit images), where after a preparation step involving to walk over the image once, the image's size does not matter any longer at all. Finally, the methods were implemented and demonstrated to give good results for different example images.

Still, there are a lot of areas open for further research. For one, I was not able to prove full convergence of the fixed-point iteration proposed or that a found result is optimal; actually, it needs not be so. But possibly further restrictions on the image processed could lead to a unique solution and full theoretical justification. And secondly, an interesting point to consider is the possibility to generalize the ideas used herein for images not necessarily gray-scale; that is, with multi-dimensional intensities instead of only $I \subset \mathbb{R}$. There, one can still define a distribution function and use it instead of the original image, but its domain will be the new, extended intensity-space instead of $\mathbb{R}$. Thus boundaries there can no longer be represented as a finite-dimensional vector. As a way out, it may be noted that Equation 13 can be interpreted to give the boundaries when segment intensities are fixed, leading to a Voronoi tessellation of the intensity-space as seen by the proof of Theorem 14. The centers instead of boundaries are still finite-dimensional even in the general case of higher-dimensional intensities. Thus this may be a way to formulate a still finite-dimensional optimization problem for such images, too.

References

[1] GNU Octave. `http://www.gnu.org/software/octave/`.

[2] Maxima. `http://maxima.sourceforge.net/`.

[3] Robert B. Ash. *Real Analysis and Probability*, volume 11 of *Probability and Mathematical Statistics*. Academic Press, New York, 1972.

[4] Gilles Aubert and Pierre Kornprobst. *Mathematical Problems in Image Processing*. Springer, second edition, 2006.

[5] Martin Barner and Friedrich Flohr. *Analysis I*. de Gruyter, New York, fourth edition, 1991.

[6] Lawrence C. Evans and Ronald F. Gariepy. *Measure Theory and Fine Properties of Functions*. CRC Press, Boca Raton, 1992.

[7] Michael Hintermüller and Antoine Laurain. Multiphase image segmentation and modulation recovery based on shape and topological sensitivity. *SFB Report*, 2008-015, 2008. Graz, Austria.

[8] Stephen L. Keeling, Michael Hintermüller, Florian Knoll, Daniel Kraft, and Antoine Laurain. A Total Variation Based Approach to Correcting Surface Coil Magnetic Resonance Images. *SFB Report*, 2010-016, 2010. Graz, Austria.

[9] David J. C. MacKay. *Information Theory, Inference, and Learning Algorithms*. Cambridge University Press, Cambridge, 2003.